# WATERCUT MEASUREMENT METHOD BY USING HIGH SPEED IMPEDANCE SENSOR

A Thesis

by

BURAK ERDOGAN

Submitted to the Office of Graduate and Professional Studies of
Texas A&M University
in partial fulfillment of the requirements for the degree of

MASTER OF SCIENCE

| | |
|---|---|
| Chair of Committee, | Gerald L. Morrison |
| Committee Members, | Devesh Ranjan |
| | Karen Vierow |
| Head of Department, | Andreas Polycarpou |

December 2014

Major Subject: Mechanical Engineering

# ABSTRACT

Oil and water mixtures are present in many applications, specifically in upstream oil production. To investigate oil-water mixture properties and to measure phase fractions, a watercut meter was developed that utilizes an electrical impedance measurement method. In this method, watercut is measured by using a newly developed algorithm that uses multiple frequencies to enhance the accuracy of the watercut measurements and to identify the mixture dispersion type. Electrical characteristics of the mixture were investigated by studying the effect of three factors, the emulsion properties, hysteresis effect, and temperature effect. The dependency of the watercut meter response to the influencing factors was reduced by implementing this developed novel method. Using this method, the uncertainty in watercut measurement from 0 to 1 watercuts was obtained to be about $\pm$3% regardless of phase distribution. The effect of the shear forces on emulsion properties was investigated for all watercuts separately. The hysteresis effect was investigated by testing from 1 to 0.3 watercuts and 0 to 0.7 watercuts. The temperature effect was investigated by testing from 29.44 ºC (85 ºF) to 23.88 ºC (75 ºF) for 1 watercut. The shear forces have significant effect on emulsion properties in ambivalent range. The hysteresis and temperature do not have significant effect on the watercut measurement method.

DEDICATION

*This work is dedicated to the God,*

*then to my father Yusuf Erdogan, my mother Azime Erdogan,*

*and my brother Serdar Erdogan.*

# ACKNOWLEDGEMENTS

I would like to thank Dr. Gerald L. Morrison for his guidance and support throughout my research. I also would like to thank to my committee members, Dr. Devesh Ranjan and Dr. Karen Vierow.

I would like to thank everyone at the TurboLab, especially Sahand Pirouzpanah, for giving me advice and helping me finish my research. I also would like to thank my roommate Yusuf Turhan for his support and patience. Thanks to Abdulkadir Bostanci, Gokhan Yildirim, and Mustafa Karabacak, for their support.

I also would like to thank TPAO for financial support throughout my master education

Finally, thanks to my father, mother and brother for all their emotional and financial support.

NOMENCLATURE

| | |
|---|---|
| $A_{ci}$ | Closed loop gain for ideal op-amp |
| $A_{or}$ | Open loop gain for ideal op-amp |
| $C_f$ | Feedback capacitance |
| $C_s$ | Stray capacitances due to the effect of the cable |
| $C_x$ | Equivalent mixture electrical capacitance |
| $R_f$ | Feedback resistance |
| $R_x$ | Equivalent mixture electrical resistance |
| $V_i$ | Input Voltage of Sensor |
| $V_o$ | Output Voltage of Sensor |
| $\beta$ | Feedback factor |
| $w$ | Angular frequency |
| $w_c$ | -3dB cut off angular frequency |
| $w_u$ | Op-amp unity gain bandwidth |
| $\varphi$ | Phase shift |

TABLE OF CONTENTS

Page

LIST OF FIGURES

Page

LIST OF TABLES

Page

# 1. INTRODUCTION*

Multiphase flow is a combination of two or more components which are solid, liquid and gas. The common types of two-phase and three-phase flows are listed below. [1]

- Gas - Solid flow
- Liquid – Liquid flow
- Liquid – Solid flow
- Gas – Liquid flow
- Gas – Liquid – Solid flow
- Gas – Liquid – Liquid flow
- Solid – Liquid – Liquid flow

Multiphase flow meters have been in use in different industries such as chemical and petroleum for many years. In the petroleum industry, two-phase flow has significant importance in production wells and pipelines. Among different two-phase flow types, liquid-liquid dispersion is commonly found in different applications and due to its importance it has been investigated by many researchers. In this study, water-oil dispersion will be investigated as liquid-liquid dispersion. [2]

---

* Parts of this thesis are reprinted with permission from "Study of Hysteresis Effects and Emulsion Properties in Watercut Measurement Using High Speed Multi-Frequency Impedance Sensor" by Sahand Pirouzpanah, Burak Erdoğan, and Gerald L. Morrison, 2014. Accepted by *Flow Measurement and Instrumentation* by Elsevier.

# 2. LITERATURE REVIEW

In two-phase water-oil flow, two types of dispersion occurs which are oil-in-water (o/w) and water-in-oil (w/o). In oil-in-water (water-in-oil) dispersion, water (oil) is the continuous phase and oil (water) is the dispersed phase which means that oil (water) droplets are in the water (oil). By changing the water volume fraction (watercut) and by energy input, during a specific phenomenon, the dispersed phase switches to the continuous phase and the continuous phase inverts to the dispersed phase. This phenomenon is called *phase inversion*. After phase inversion, oil droplets in water invert to water droplets in oil and vice versa. [2]

The phase inversion was observed to occur for a specific range of watercut values. Water is the continuous phase for higher watercuts and oil is the continuous phase for lower watercuts. Between these two limits there is a range that either phase can be stably continuous. This region is called *ambivalent range* [3]. The ambivalent range shows the hysteresis effect presence [4]. Phase inversion from oil-in-water to water-in-oil dispersion and water-in-oil to oil-in-water dispersion represents the hysteresis phenomenon [1,5]. The procedure at the beginning of the dispersion determines which phase will be continuous [3]. The ambivalent range width depends on how the dispersion is produced [6].

Various parameters which affect the phase inversion and ambivalent range have been investigated in an agitated tank by different researchers [2,3,5,6,7,8]. The impeller size [5,8], tank impeller diameter ratio [5], and density difference of liquids [5,7,8] do

not have important effect on the ambivalent range. Ambivalent range narrows by increasing the agitation speed [2, 6]. According to Norato et al interfacial tension has a significant effect on ambivalent range [5]. The ambivalent range is a function of viscosity ratio which has significant effect on ambivalent range and phase inversion [3,5,7,8].

Phase inversion is defined by coalescence and breakup imbalance [8,9]. It is found that the coalescence rate is higher than breakup rate in the phase inversion region [8]. Therefore, droplet size increases significantly before the phase inversion because of the high coalescence rate [2,9]. Also, it is found that the phase inversion process occurs gradually and locally within the mixture [2].

The secondary dispersion water-in-oil-in-water (w/o/w) is rarely observed before phase inversion. The oil-in-water-in-oil (o/w/o) dispersion is observed during and after phase inversion. Increasing the stirrer speed after phase inversion decreases the o/w/o dispersion. Two large oil drops collide and the small oil drop, which is surrounded by water, covered by large oil drop. Coalescence of the large oil drop is concluded with water in oil emulsion. The secondary droplet of oil in water in oil (o/w/o) occurred. [2]

Although viscosity and density of two dispersion types in an oil-water mixture are identical, dielectric constant of oil-in-water and water-in-oil are different [10].

In the watercut meter industry, different methods have been in use such as near-infrared technique (NIR) [11], microwave method [12], gamma tomography [13], and impedance measurements [14]. The impedance measurement method uses the impedance variation of the oil-water mixture for different water contents to obtain the

watercut. There are different types of sensors and configurations that are in use for impedance measurements such as stripe, ring [15], cylindrical [14] and six electrodes configuration [16].

The impedance method is applicable for both gas-liquid mixture and liquid-liquid emulsion [1]. In the Turbomachinery Laboratory at Texas A&M University, the impedance measurement method was used for gas volume fraction measurement in the gas-liquid (air-water) mixture employing two impedance electrodes and a slotted orifice plate as the flow conditioner and homogenizer [17]. In this study, a similar sensor but with higher excitation frequencies was implemented to measure the watercut in oil-water emulsions in an agitated vessel.

# 3. OBJECTIVES

In two-phase oil pipelines, due to the presence of valves, bends and flow conditioners, the emulsion properties of the oil-water mixture changes. To reduce the dependency of electrical response of the impedance sensor to the upstream conditions, the electrical characteristic of the mixture for different emulsion properties was investigated in this study.

The emulsion properties vary as a result of changing the volume fraction of the mixture and agitation or applying shear forces to the mixture. To investigate the emulsion properties, the mixture at specific watercut was agitated for different durations of time. The electrical response of the sensor to the variation of emulsion properties by time was recorded.

By using the response of multi-frequency impedance sensor along with a newly developed algorithm, detailed mixture characterization is performed. Also, resistance and capacitance of the mixture is calculated. In addition, hysteresis and temperature effects are studied in order to investigate their influence on the accuracy and performance of the watercut meter.

# 4. EXPERIMENTAL MATERIALS AND METHODS

In this section, experimental setup, procedure, and mixture resistance and capacitance calculation are provided.

## 4.1. Experimental Setup

The test section is shown in Fig. 1. In this test section, a 48.6 mm diameter agitated vessel was used to mix two immiscible liquids. The liquids were chosen to be tap water and vegetable oil. The selection was made based on availability and ease of disposal. The agitated vessel includes an impeller with four blades that are 24 mm long. Liquids were mixed in a 30.5 cm long vertical clear PVC pipe. Two ultra-machinable brass impedance sensors (Fig. 2) were flush mounted to the pipe across from each other. The sensors at their contact points with the fluid mixture have the diameter of 17 mm.

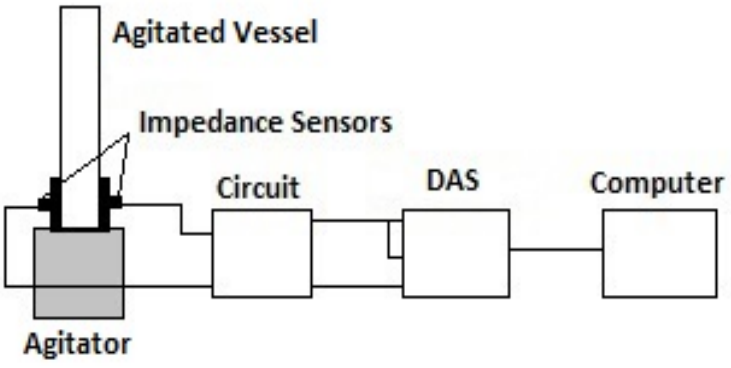


**Figure 1.** Schematic representation of experimental setup

**Figure 2.** Electrical impedance sensor

The electrodes were connected to the circuit by using RG 58/U type coaxial cables. The circuit is shown in Fig. 3. In the circuit, 'Texas Instrument - LM7171' op-amp was used in the shown configuration. A power supply was used to apply 15V DC voltage to the op-amp. In the circuit, $R_x$ and $C_x$ represent the resistance and capacitance of the mixture, respectively. $R_f$ and $C_f$ are the feedback resistance and capacitance. $C_{s1}$ and $C_{s2}$ are the stray capacitances due to the effect of the cables. The lengths of the cables were kept as short as possible to decrease the stray capacitance effect on the circuit performance.

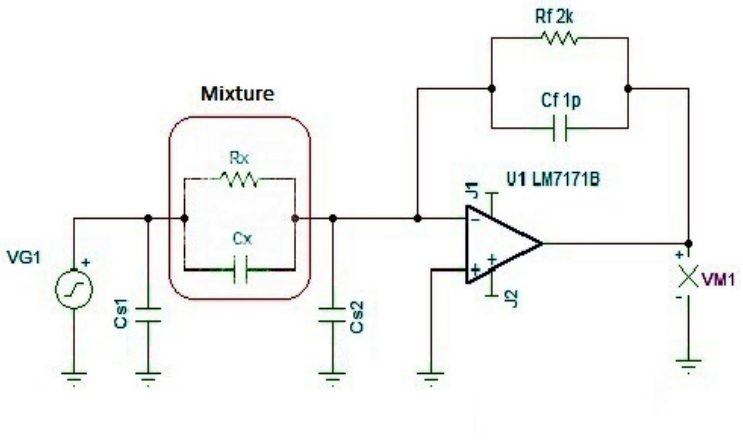


**Figure 3.** Schematic representation of the circuit

Twelve sinusoidal signals with different frequencies ranging from 0.2 to 10 MHz and similar amplitude were combined and applied as the input signal to the circuit. A Picoscope–5242B was used as a signal generator and data acquisition system. The Picoscope has two input channels and one output channel. The output channel was connected to the input of the circuit and one of the inputs of the Picoscope. Other input channel of the DAS was connected to the output of the circuit. The output, input voltage, and phase shift measured by the DAS. The gain is fraction of output voltage to input voltage. The Labview interface (Fig. 4) was used to display and record the input and output waveforms. In the Labview, a FFT program which has real and imaginary portions was used to obtain input and output voltage and phase. The voltages are extracted from the amplitude of the complex value at a given frequency and the phase is the result of the FFT at a given frequency.

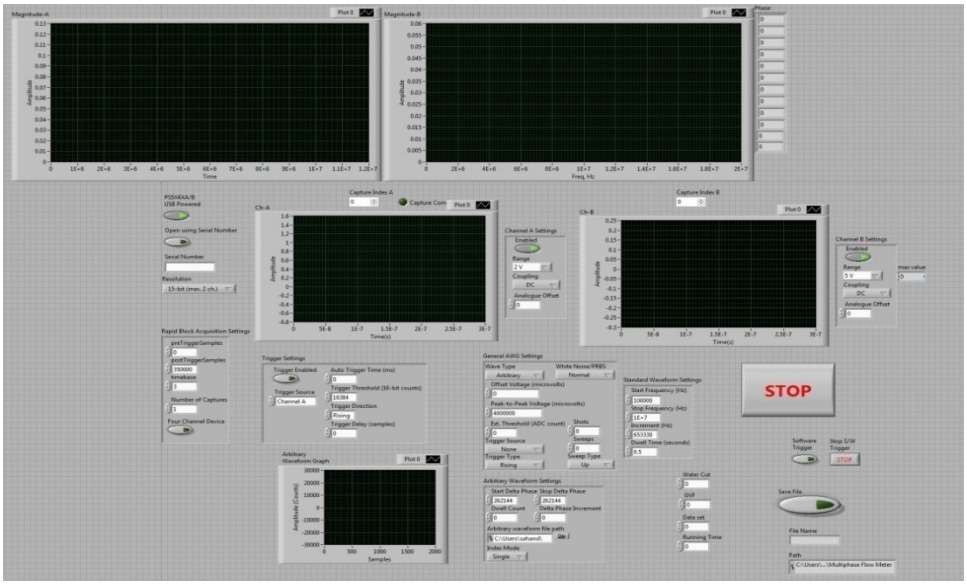


**Figure 4.** Labview interface for the experiment

The experimental setup is shown in Fig. 5. In this compact design, DAS, circuit, and two power supplies are mounted in a box. The design advantages are listed below.

- Portable
- Cheap
- Easy to setup
- Wireless connection to recording device

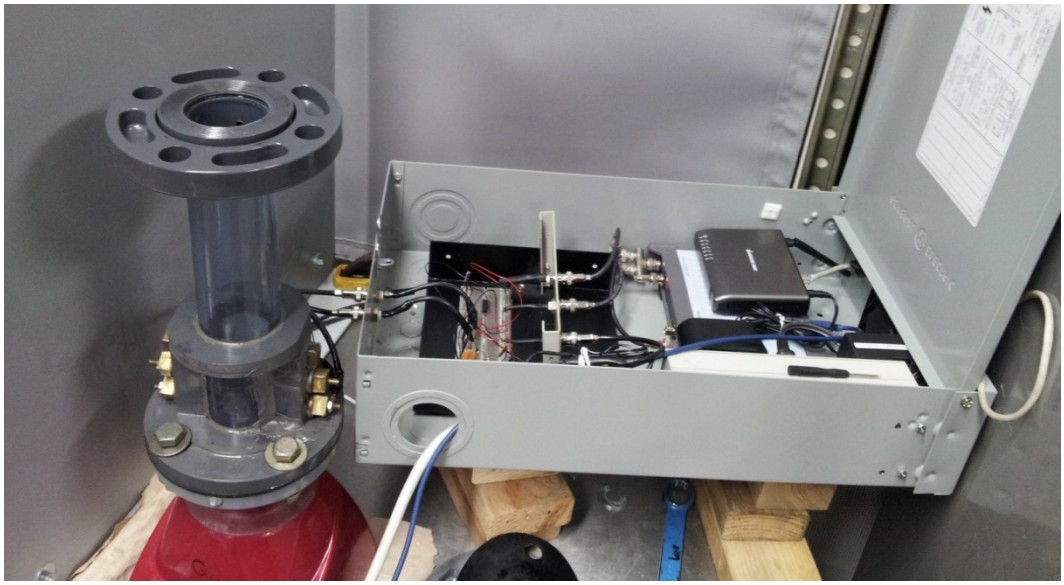

**Figure 5.** Experimental Setup

## 4.2. Experimental Procedure

In this section, detail descriptions about the experiments are provided. Three types of studies were performed. First, emulsion properties of the mixtures were investigated. Emulsion properties were varied by agitating and applying shear forces to the oil-water mixture. This process changes the droplet size, the dispersed phase

distribution and electrical mixture properties. To study the effect of emulsion properties on the sensor response, water-oil mixture for different watercut values were mixed in a 48.6 mm diameter agitated vessel for different durations of time. The duration of mixing process varies the droplet size and the distribution of the dispersed phase. To initiate the experiments, the non-emulsified samples with different watercut values were prepared separately. The total volume of each sample was set as 200 ml and agitation speed was kept fixed at 777 rpm for all watercuts. While the mixture was agitated for different durations of time, the input, output signal voltage, and phase difference between output and input signals were recorded.

The other factor affecting the impedance measurements in water-oil mixtures is the hysteresis effect. Sensor responds differently when oil as the dispersed phase is added to the mixture and, conversely, when water as the dispersed phase is added to the mixture. In this test, the samples for different watercuts were not prepared separately. Initially, specific amount of water was added into the vessel. Then, different watercut values from 1 to 0.3 were reached by gradually adding oil into the mixture. During this process the water phase remained as the continuous phase. To change the continuous phase to oil, the test was initiated and oil was used as the continuous phase instead. Different watercut values from 0 to 0.7 were obtained by gradually adding water into the vessel. In this test, mixing time was kept at 10 seconds for all watercuts. The agitation speed kept constant at 777 rpm.

Temperature is another factor which can affect the measurement. In this experiment, 200 ml water was added into agitated vessel at 29.44 ºC (85 ºF)

temperatures. Then, the data was saved for different temperatures until 23.88 ºC (75 ºF), while the water was cooling naturally. The important point is about the thermocouple. If the thermocouple is connected to mixture, the data will be wrong, so the thermocouple was not connected to the agitated vessel. It was removed while recording the data.

### 4.3. Mixture Resistance and Capacitance Calculation

In this section, the mixture resistance and capacitance calculation method is explained. The objective is to obtain the corresponding transfer function of the circuit to calculate unknown parameters in the circuit ($R_x$ and $C_x$). The $C_{s1}$ does not affect the measurement, since it is derived directly by the voltage source. $C_{s2}$ has little effect on the sensor response. The real op-amp closed loop gain ($A_{cr}$) is calculated by eq.1 [18,19].

$$A_{cr} = \frac{V_o}{V_i}(\cos\varphi + i\sin\varphi) = \frac{A_{ci}}{1 + \frac{1}{A_{or}\beta}} \tag{1}$$

The closed loop gain for ideal op-amp ($A_{ci}$) is calculated by neglectingthe $C_{s2}$ [18,19].

$$A_{ci} = -\frac{R_f + jwC_xR_xR_f}{R_x + jwC_fR_fR_x} \tag{2}$$

The open loop gain for the real op-amp ($A_{or}$) calculation is shown in eq. 3 [18,19].

$$A_{or} = \frac{1}{\frac{1}{A_o} + \frac{jw}{A_o w_c}} \tag{3}$$

The op-amp unity gain bandwidth ($w_u$) is the product of open loop DC gain ($A_o$) and -3dB cut off angular frequency ($w_c$). Since the $w \gg w_c$, the eq. 3 becomes eq. 4 [18,19].

$$A_{or} = \frac{w_u}{jw} \tag{4}$$

The feedback factor ($\beta$) is calculated as eq. 5 by considering $C_{s2}$ parallel to$C_x$.

$$\beta = \frac{R_x(1 + jwC_fR_f)}{(R_f + R_x) + jwR_xR_f(C_x + C_{s2} + C_f)} \tag{5}$$

When the eqs. (2, 4, 5) substituted into the eq (1), $A_{cr}$ is obtained by eq. 6. The K and L variables are shown in eq. 7 and 8 respectively.

$$A_{cr} = \frac{\left(\frac{R_fK}{R_x} + LwC_xR_f\right) + j\left(KwC_xR_f - \frac{LR_f}{R_x}\right)}{K^2 + L^2} \tag{6}$$

$$K = 1 - w^2\left(\frac{R_f(C_x + C_{s2} + C_f)}{w_u}\right) \tag{7}$$

$$L = w\left(\frac{1 + \frac{R_f}{R_x}}{w_u} + C_fR_f\right) \tag{8}$$

Eq. 6 is useful for lower than 1.28 MHz frequency range. This equation was verified by using unknown fixed resistances and capacitances. Table 1 shows two results for two sets of constant resistance and capacitances. The first row is the calculation results for 1 kΩ and 22 pF and the second row is for 1 kΩ and 32 pF.

**Table 1.** Verification in R and C calculation

| **Frequency (MHz) / Set Values** | **0.2** | **0.3** | **0.4** | **0.5** | **0.6** | **0.7** | **0.8** | **1** | **1.28** |
|---|---|---|---|---|---|---|---|---|---|
| **1(kΩ)** | 1 | 1 | 1 | 1 | 1 | 1 | 1 | 1 | 0.99 |
| **22(pF)** | 21.4 | 20.4 | 20.2 | 20.1 | 20 | 20 | 20 | 19.3 | 20.7 |
| **1(kΩ)** | 1 | 1 | 1 | 1 | 1 | 1 | 1 | 0.99 | 0.99 |
| **32(pF)** | 31.1 | 30.2 | 29.9 | 29.8 | 29.8 | 29.7 | 29.7 | 29 | 30.4 |

By substituting the measured input and output voltages, and phase shift in eq. 6, for each different frequency from 0.2 to 1.28 MHz, $R_x$ and $C_x$ are calculated.

# 5. RESULTS

In this section, experimental results are described. First, watercut measurement method and calculation steps are explained, then resistance and capacitance calculation results for the mixtures are shown, and finally hysteresis effect on the watercut measurement is investigated.

## 5.1. Emulsion Properties

The experimental results of 0.2, 0.5, and 0.8 watercuts are shown in Figs. 6-9. Fig. 6 represents the gain changes by frequency for different mixing times. The gain is used as magnitude rather than complex quantity in figures. According to this figure, by increasing the watercut, the gain of the circuit increases. It is due to the higher conductivity and permittivity of the water with respect to the oil. Fig. 7 shows the gain change by mixing time for different frequencies. The type of phase distributions for 0.2 watercut is considered to be water-in-oil whereas for 0.8 watercut is considered to be oil-in-water. However, 0.5 watercut demonstrates both phase distributions for different mixing times. For 0.5 watercut value, at low mixing times, oil-in-water phase distribution was observed, and then at high mixing times phase inversion occurred and water-in-oil phase distribution was observed. The phase inversion was observed to occur for 0.3, 0.4, 0.5, and 0.6 watercut values. These results show that the ambivalent region of the water and oil is from 0.3 to 0.6 watercuts. The existence of ambivalent range agrees with the literature [3].

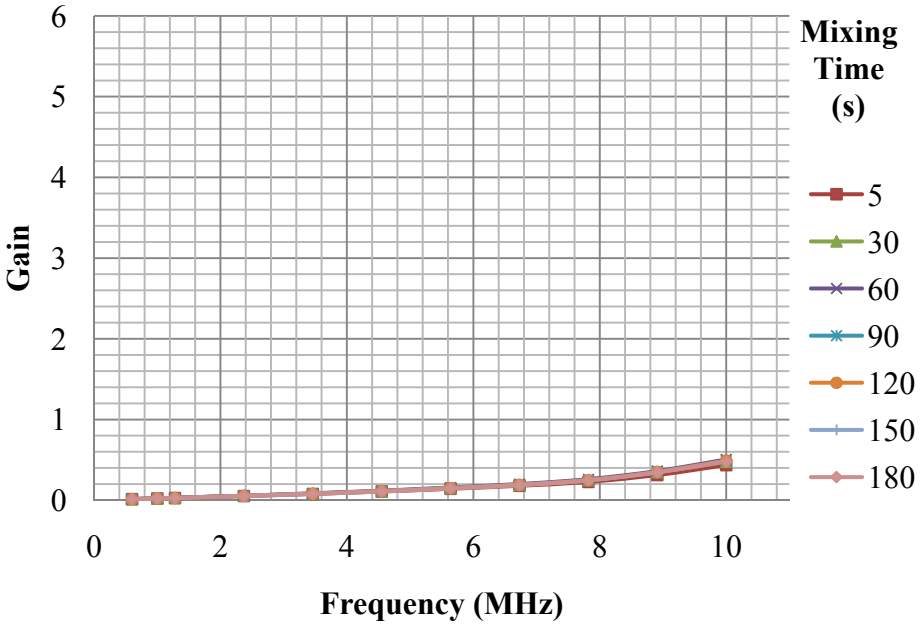


(a)

**Figure 6.** Gain variation with frequency for different mixing times (a) 0.2 (b) 0.5 and (c) 0.8 watercut

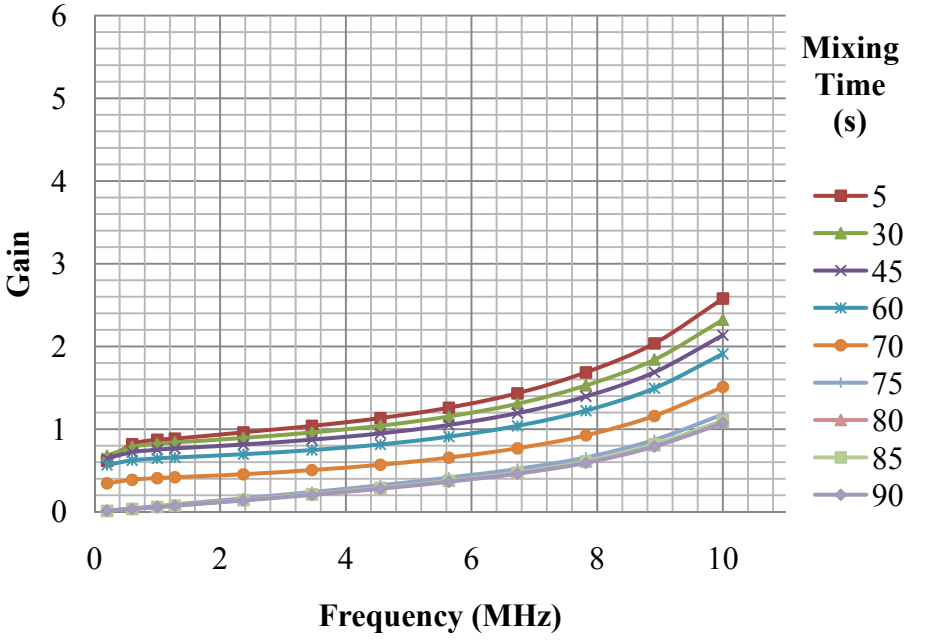


(b)

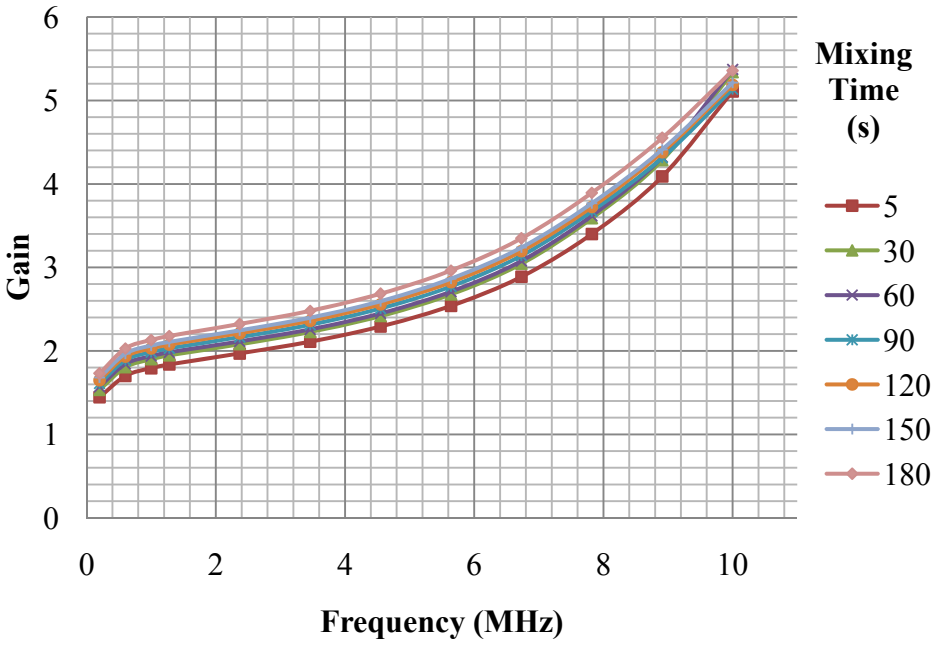


(c)

**Figure 6.** Continued

The gain variation with respect to the mixing time is noticeable especially for the ambivalent range whereas for the rest of the watercut values it is approximately constant. The watercuts in ambivalent range show dependency on mixing time. In the ambivalent range, the oil droplets coalesce and bigger oil droplets form before the phase inversion. By increasing the oil droplet size, the conductivity of the mixture decreases. Therefore, the gain decreases by further agitation of the emulsion.

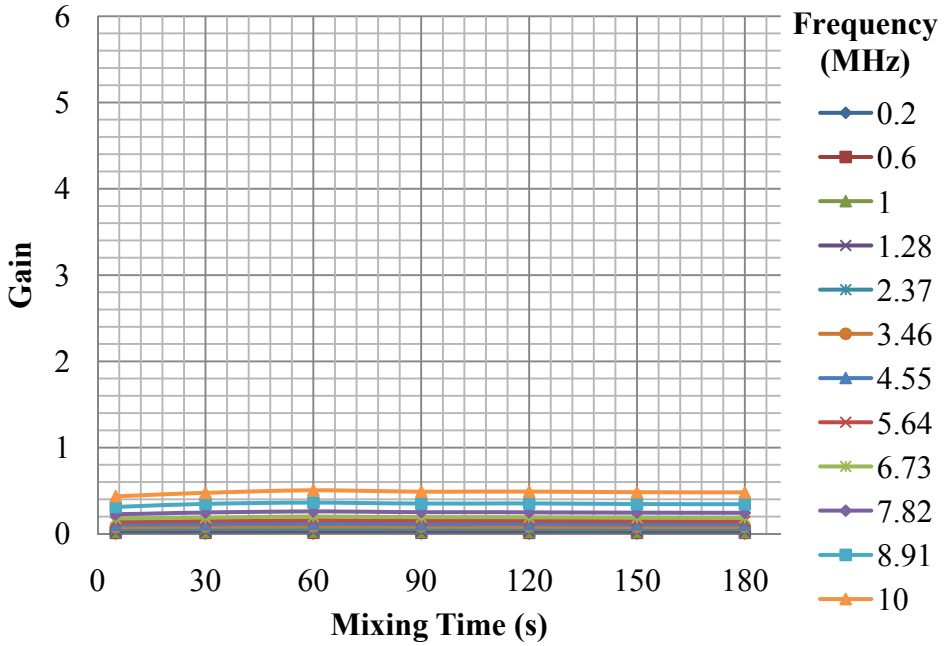


(a)

**Figure 7.** Gain variation by mixing time for different frequencies (a) 0.2 (b) 0.5 and (c) 0.8 watercut

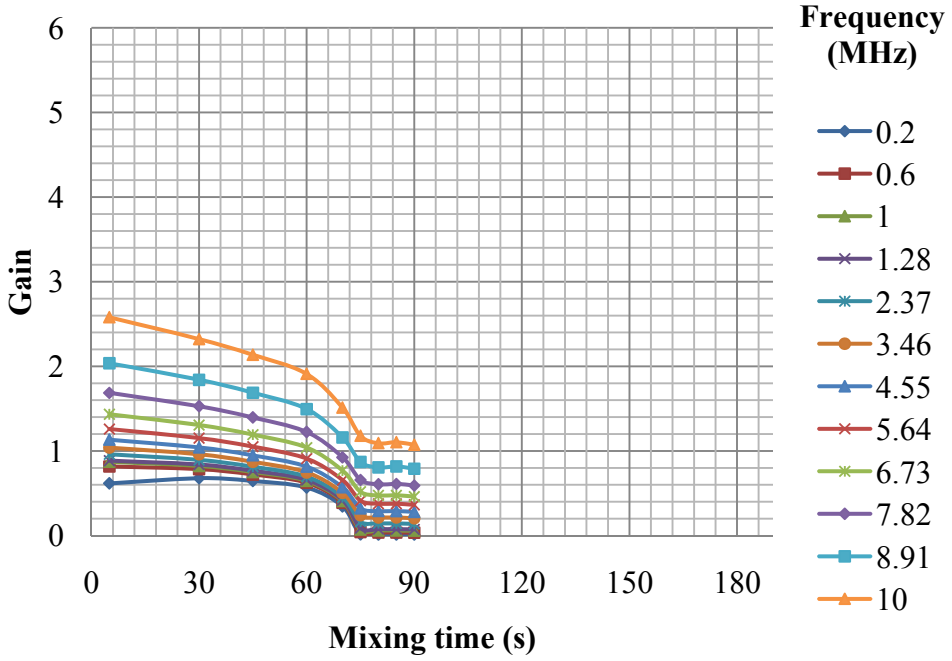


(b)

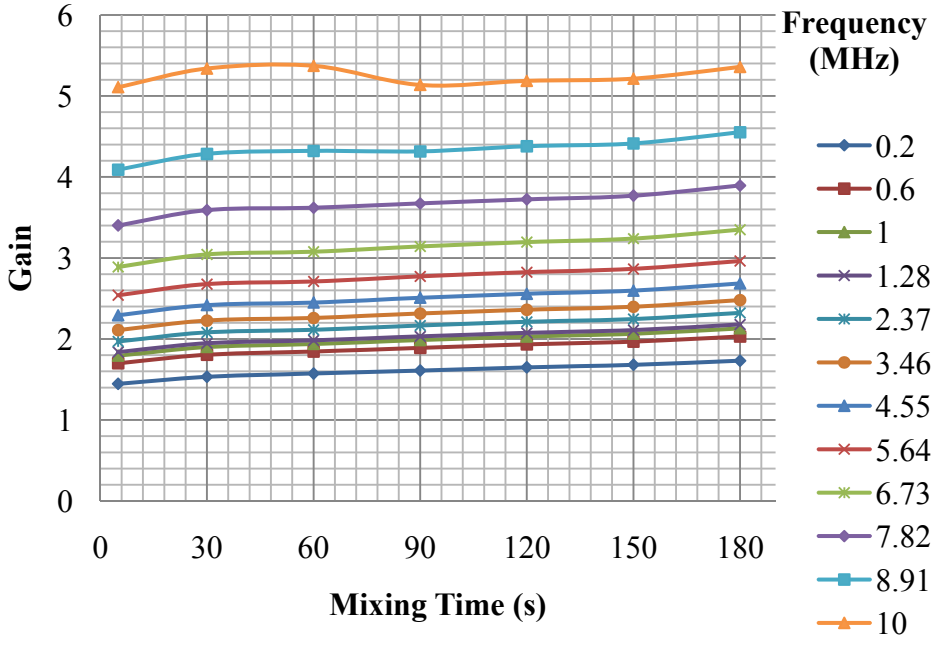


(c)

**Figure 7.** Continued

The gain variations with frequency for all watercuts at five second mixing time results are shown in Fig. 8. The graph shows that gain values are increasing by watercuts; however, the gap between 0.4 and 0.3 watercuts is wider than the other gaps. The reason is the different dispersion type. Water-in-oil dispersion is observed from 0 to 0.3 watercut where the gain values are low and oil-in-water dispersion was observed for the rest of watercuts.

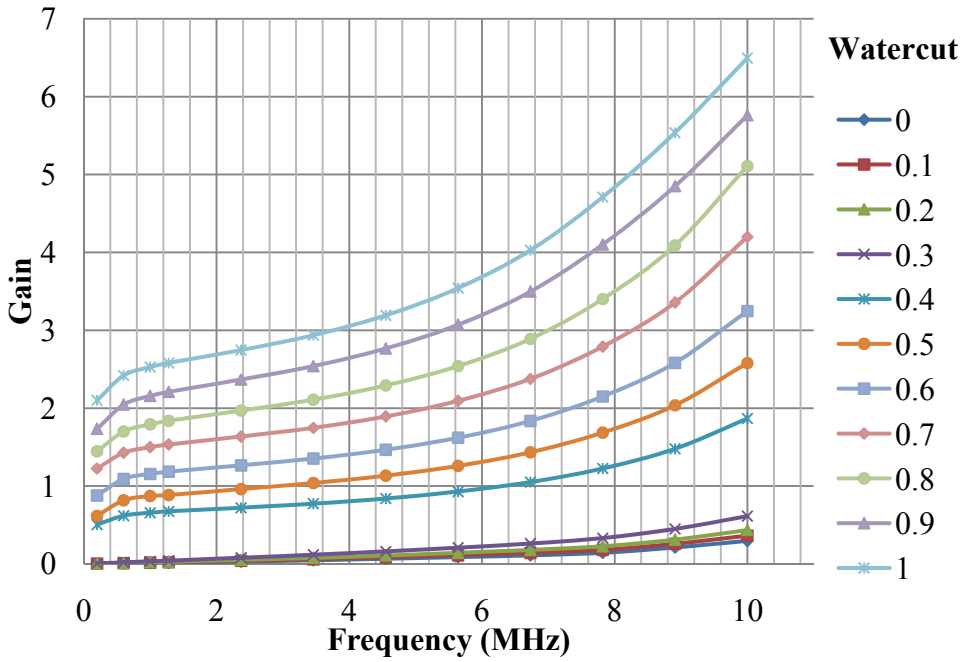


**Figure 8.** 5 second results for all watercuts

The phase shift variation by frequency for different mixing times results are shown in Fig. 9. The phase shift is the phase difference between outlet signal and inlet signal of the circuit. The phase shift is decreases with frequency for oil-in-water and

water-in-oil dispersion and the decreasing amount for oil-in-water is higher than water-in-oil dispersion. The other important point is that the phase shift values of oil-in-water values are lower than water-in-oil values.

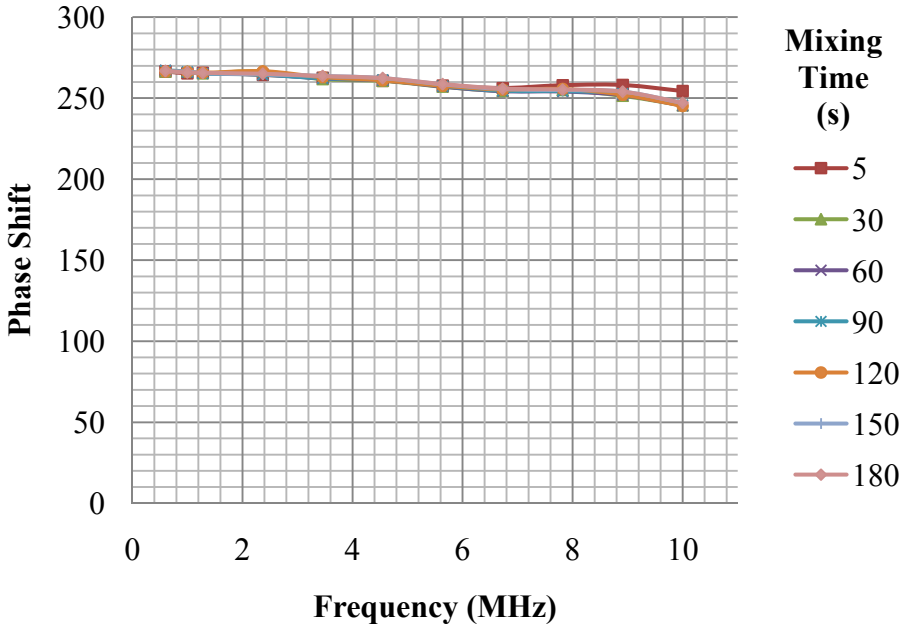


(a)

**Figure 9.** Phase shift variation with frequency for different mixing times at a) 0.2 b) 0.5 and c) 0.8 watercut

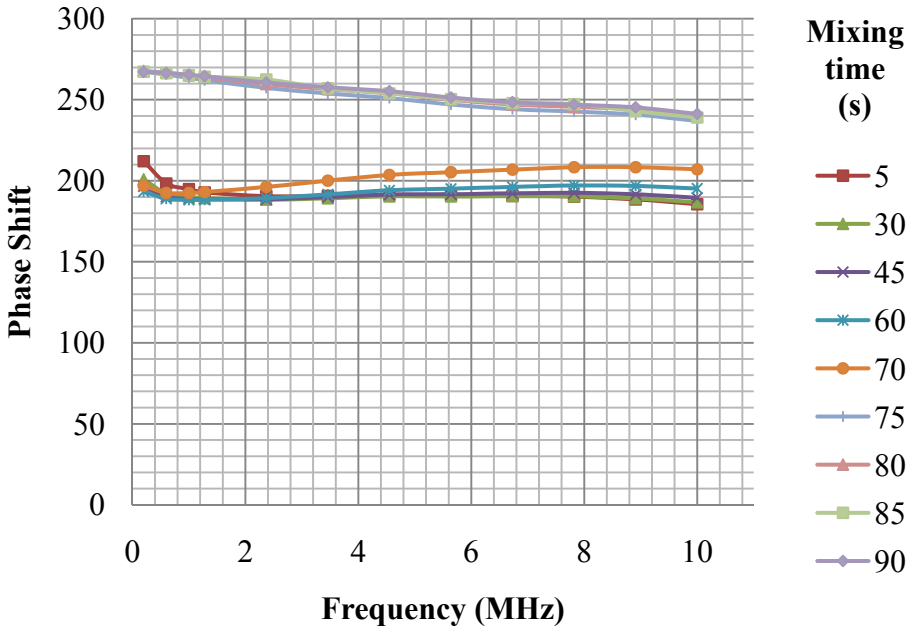


(b)

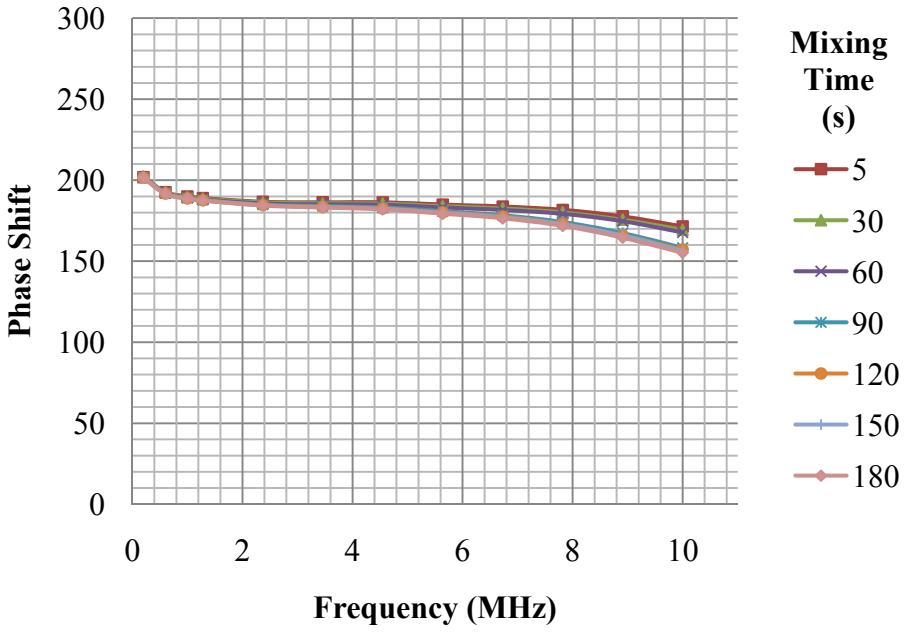


(c)

**Figure 9.** Continued

The phase shift variation with mixing times for different frequencies is represented in Fig. 10. The phase shift values are constant by mixing times except in the ambivalent range. In the ambivalent range, the oil-in-water values are lower than water-in-oil values. The phase shift values for oil-in-water (water-in-oil) dispersion for all watercuts are about the same.

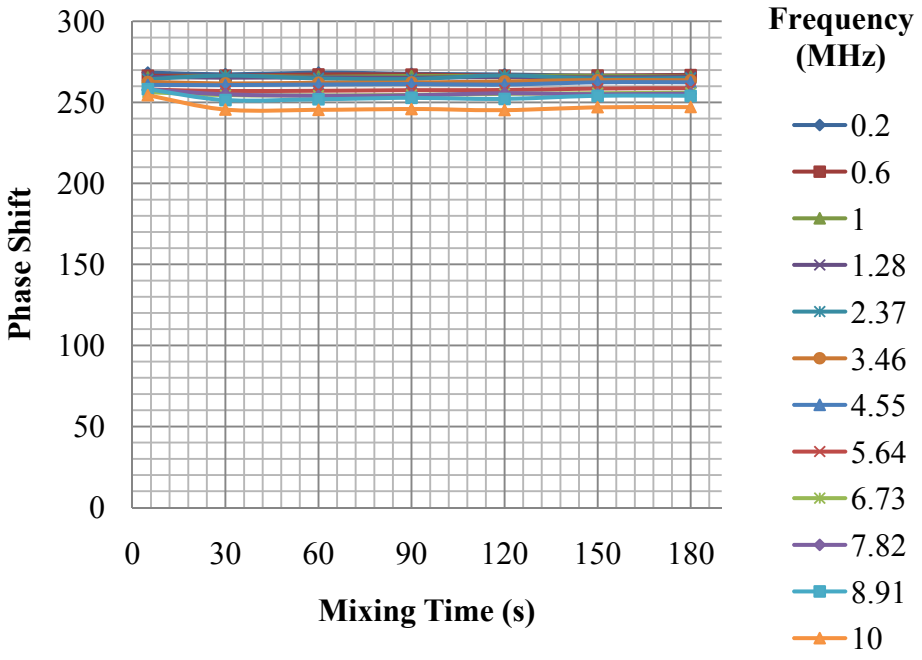


(a)

**Figure 10.** Phase shift variation by mixing time for different frequencies at a) 0.2 b) 0.5 and c) 0.8 watercut

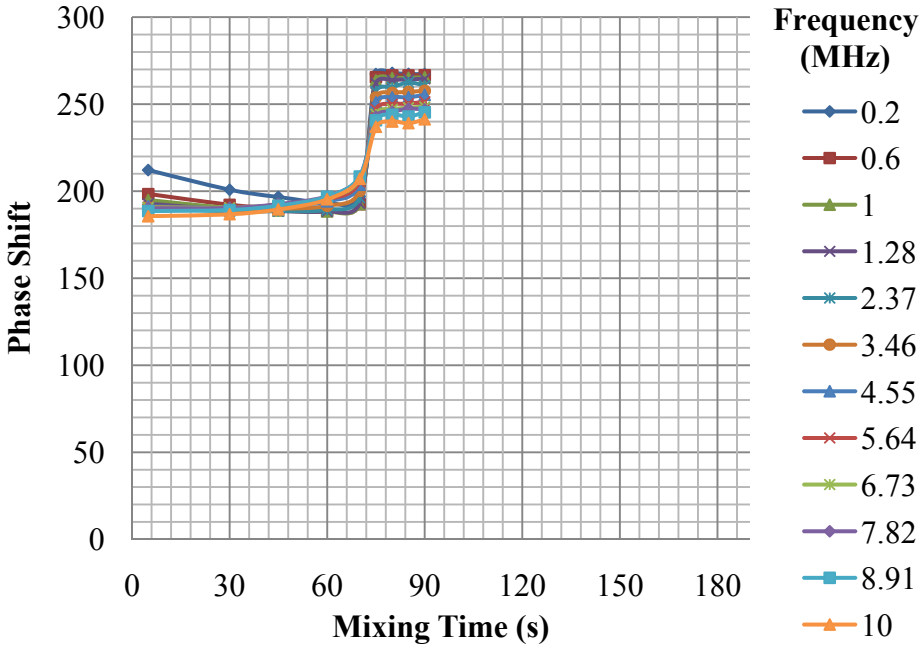


(b)

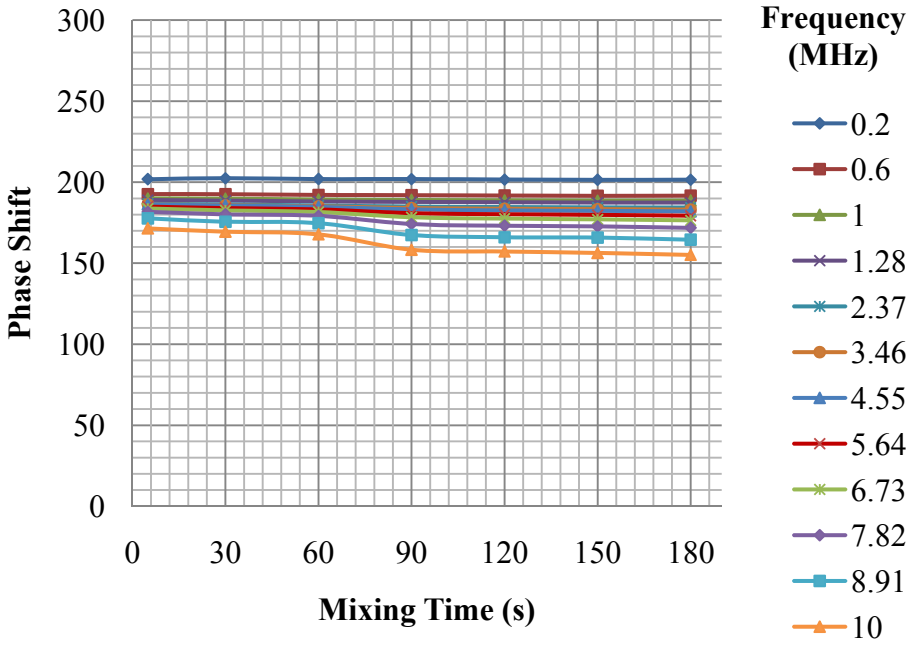


(c)

**Figure 10.** Continued

The phase inversion was observed at different mixing times for different watercuts in the ambivalent range. The phase inversion occurrence times are presented at Table 2. The time, when the phase inversion occurs, increases with increasing the watercut.

**Table 2.** Phase inversion occurrence time for different watercuts

| **Watercut** | 0.3 | 0.4 | 0.5 | 0.6 |
|---|---|---|---|---|
| **Time (s)** | 2-3 | 40-45 | 70-75 | 140-145 |

In this experiment, mixing time represents the amount of shear forces which are applied to the mixture by the agitator. The results show that the emulsion properties are not affected by shear forces for higher and lower watercuts. However, in the ambivalent range, shear forces have significant effect on the emulsion properties. The dispersion type was changed during the phase inversion process. During this process, continuous phase was inverted from water to oil. In addition, the electrical conductivity and permittivity increases by increasing the watercut.

### 5.2. Watercut Measurement Method

To decrease the dependency of the sensor response to the mixing time, a new parameter was introduced using the gains associated with multiple frequencies. The parameter is defined as *Gain Subtraction for Different Frequencies* (GSDF). The parameter is given in eq. 9.

$$GSDF = \left((G_{6.73MHz} - G_{3.46MHz}) - (G_{2.37MHz} - G_{0.6MHz})\right) \quad (9)$$

This parameter was applied for all watercuts and the results are presented in Figs. 11-13. Fig. 11 shows the average values for oil-in-water and water-in-oil phase distributions. To increase the accuracy of the measurements, 0.4, 0.5, and 0.6 watercut experiment results are evaluated separately as oil-in-water and water-in-oil. Figs. 12 and 13 display the average GSDF values along with the maximum and minimum values in different watercuts for water-in-oil and oil-in-water phase distributions. The difference between maximum and minimum of GSDF values are higher for oil-in-water phase distribution than water-in-oil phase distribution.

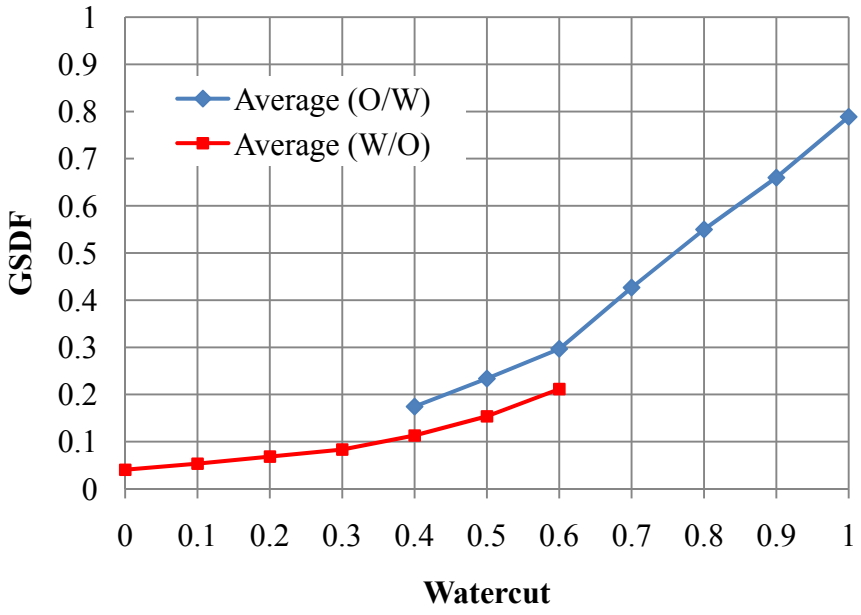


**Figure 11.** GSDF for different watercuts

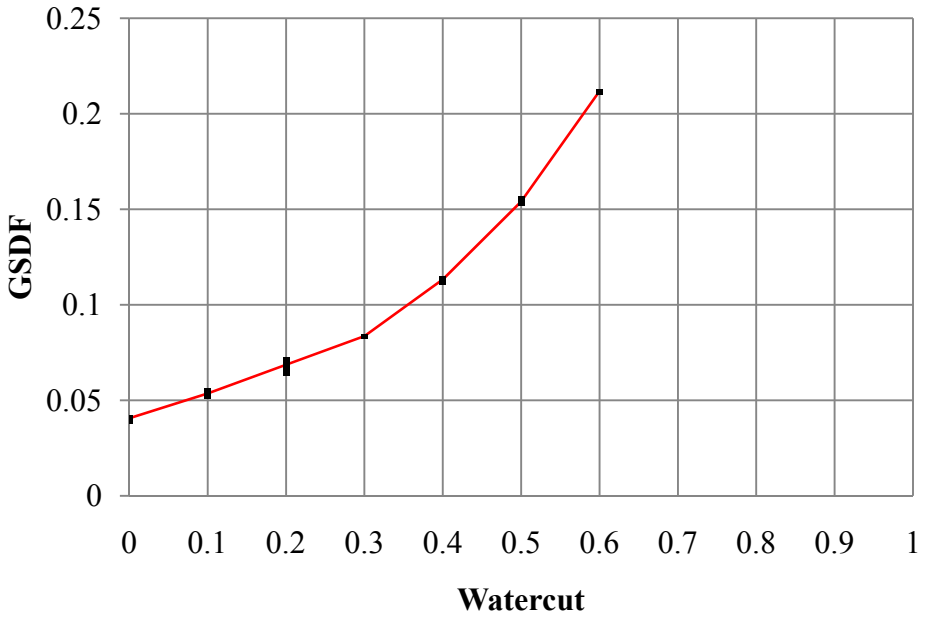


**Figure 12.** Water-in-oil, GSDF for different watercuts

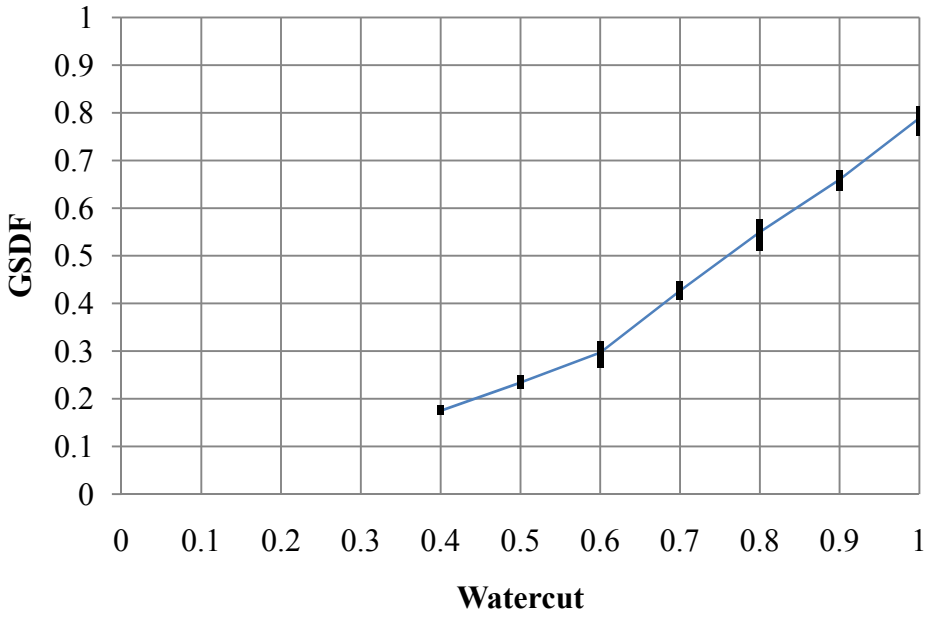


**Figure 13.** Oil-in-water, GSDF for different watercuts

To predict the watercut, two different equations are needed based on the experimental results. Curve fitting is applied for water-in-oil and oil-in-water data separately and results are shown in Fig. 14 and 15 respectively. The equations are given in eqs. 10 and 11.

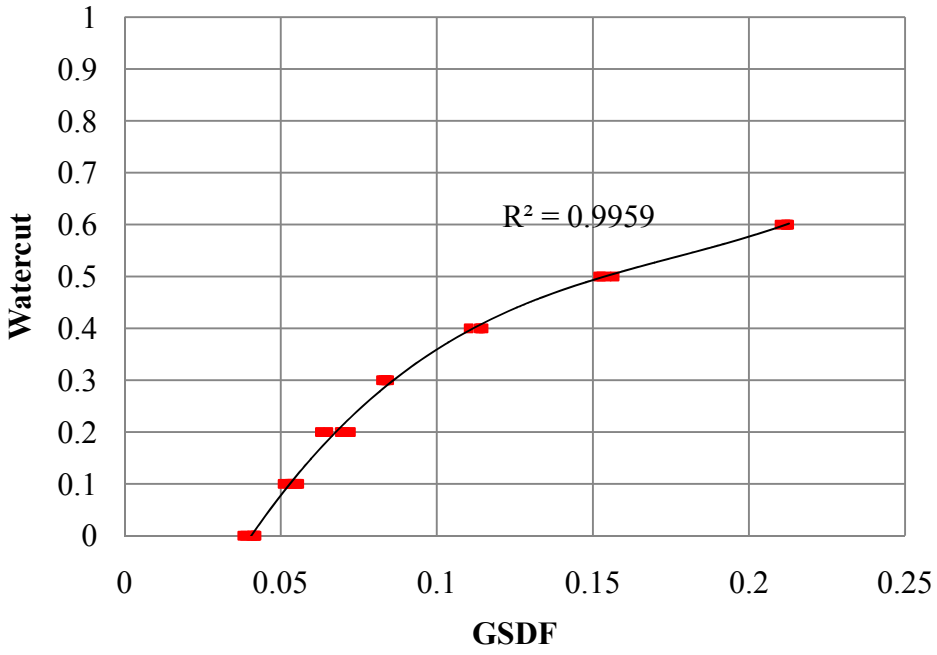


**Figure 14.** Curve fitting for water-in-oil GSDF values

$$Watercut_{w/o} = 129.8\, GSDF^3 - 68.46\, GSDF^2 + 13.63\, GSDF - 0.449 \quad (10)$$

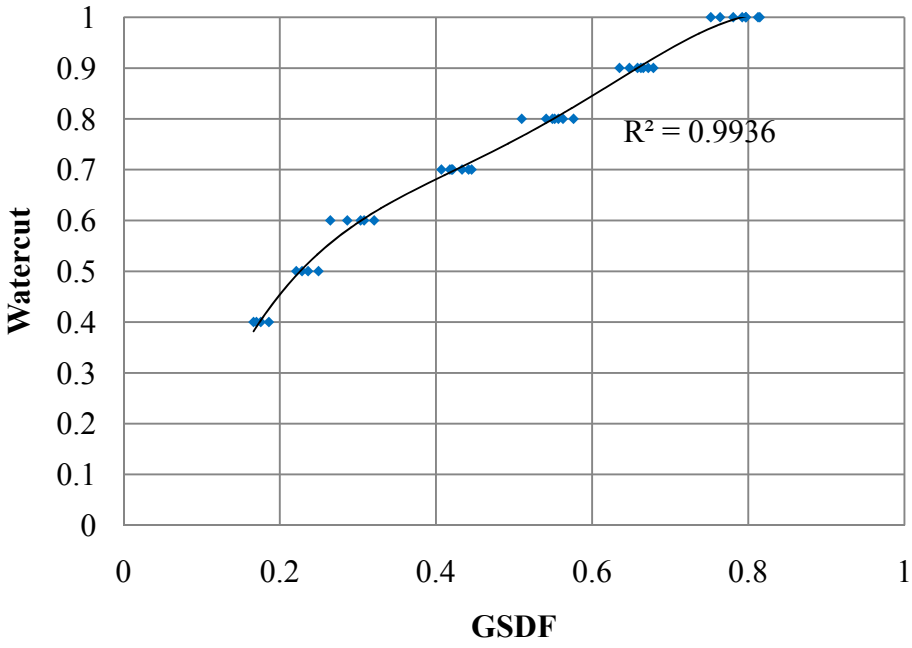


**Figure 15.** Curve fitting for oil-in-water GSDF values

$$Watercut_{o/w} = -11.1\ GSDF^4 + 23.39\ GSDF^3 - 17.75\ GSDF^2 + 6.569\ GSDF - 0.319 \quad (11)$$

To determine the proper equation in obtaining the watercut value, a constraint was defined. The corresponding gain at 0.6 MHz frequency was used as the comparing constraint. A threshold value of 0.2 was chosen for the purpose of comparison which is shown in Fig. 16 along with the corresponding phase of the original signal. When the corresponding gain at 0.6 MHz gain is lower than the threshold value, eq. 10 was used otherwise eq. 11 was implemented instead. A threshold phase value of 220 produces the same result.

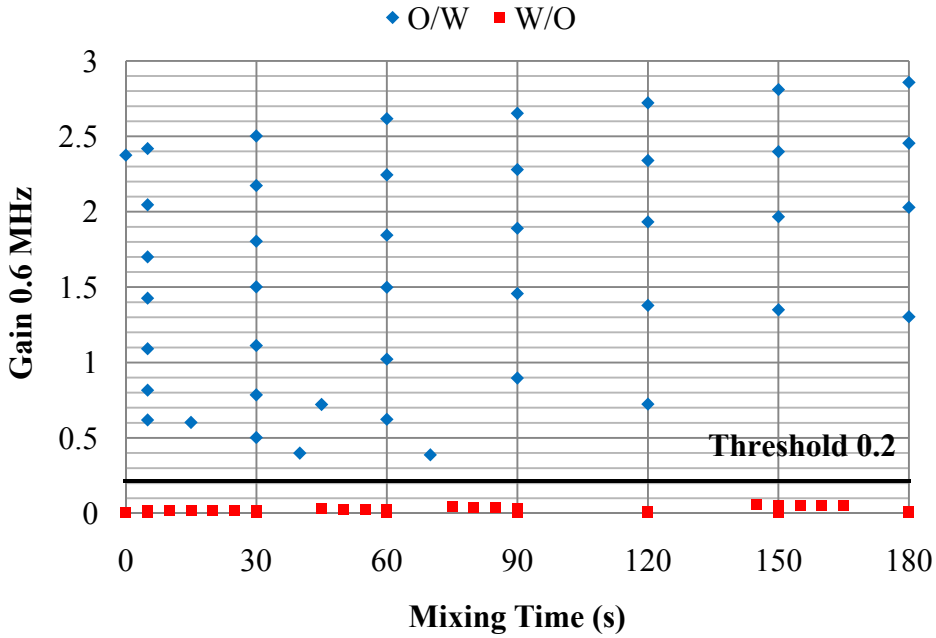


(a)

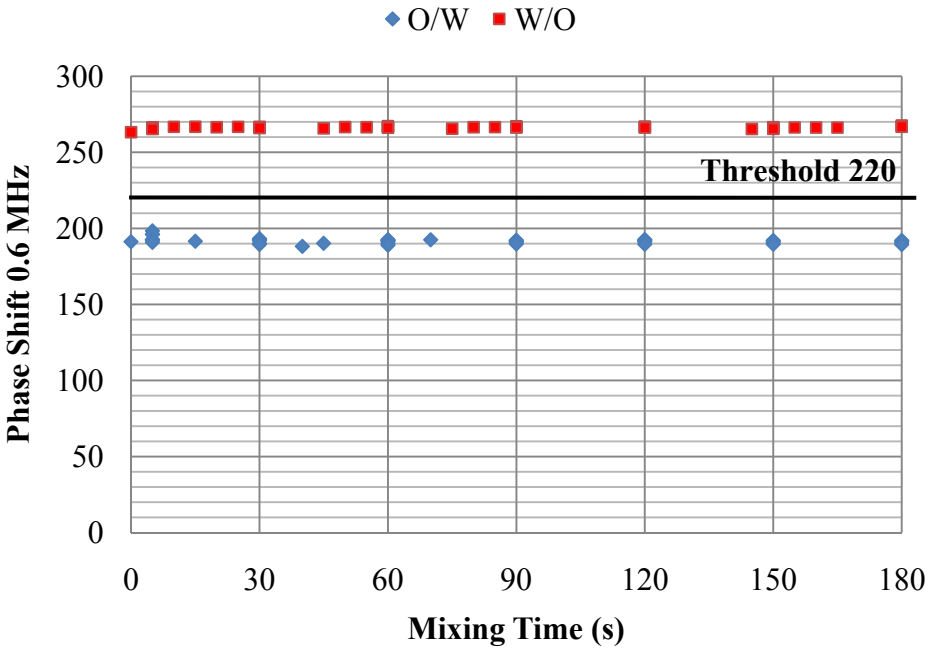


(b)

**Figure 16.** 0.6 MHz (a) Gain and (b) Phase shift results for all watercuts

To measure the watercut, an algorithm is required to be followed. First, the dispersion type needs to be identified. This is performed by comparing the gain at 0.6 MHz with the threshold value. Then, according to the dispersion type, the proper equation is employed to calculate the watercut value.

The threshold value frequency is defined as the lowest frequency in the GSDF calculation and it provides the clear evaluation. The gain threshold method with 0.3 is applicable for low frequencies from 0.6 to 2.37 MHz which is shown in Fig. 17. The phase shift threshold value 220 is applicable for all frequencies which is shown in Fig. 18.

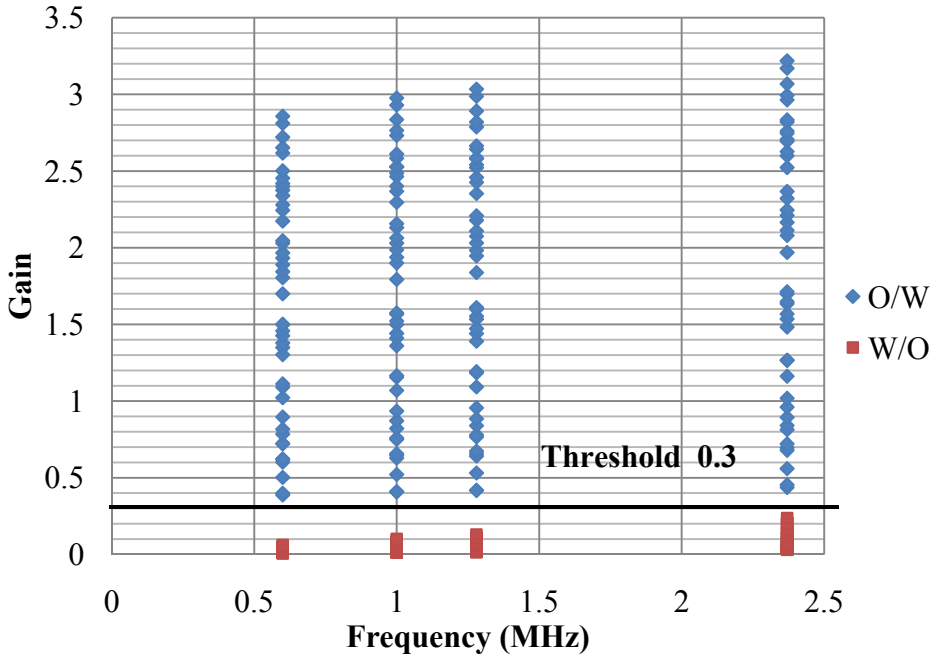


**Figure 17.** Gain threshold for all watercuts with some frequencies

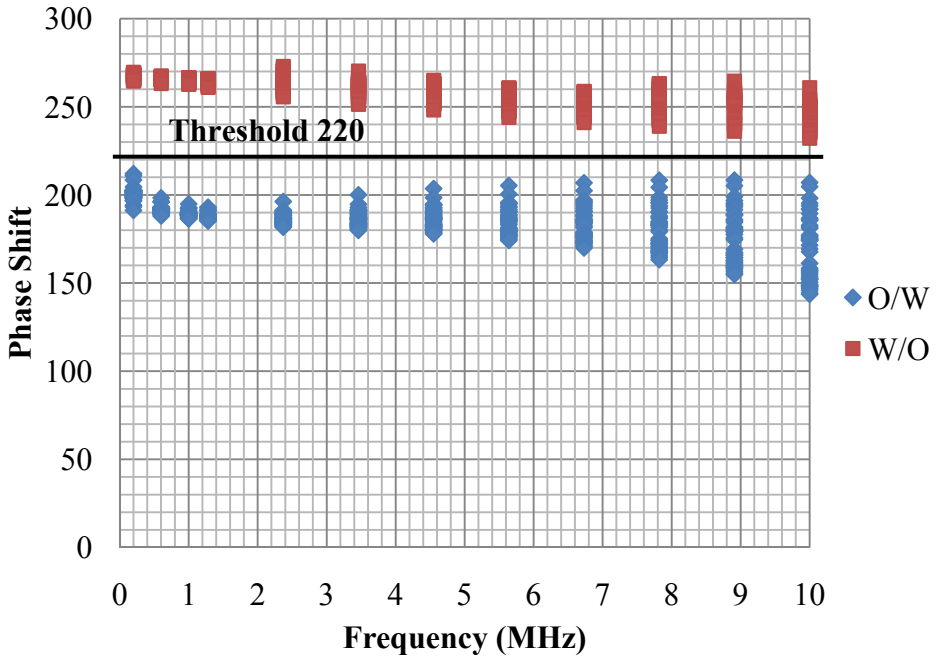


**Figure 18.** Phase Shift threshold for all watercuts and frequencies

The aforementioned method in calculating watercut was verified by comparing it with the experimental data. The difference between calculated watercut and measured watercut are shown in Figs. 19 and 20. The standard deviation of the calculated and measured watercut difference is 0.013 for water-in-oil and 0.0155 for oil-in-water calculation. The resulted uncertainty in watercut measurement was found to be about ±2.6% for water-in-oil and ±3.1% for oil-in-water.

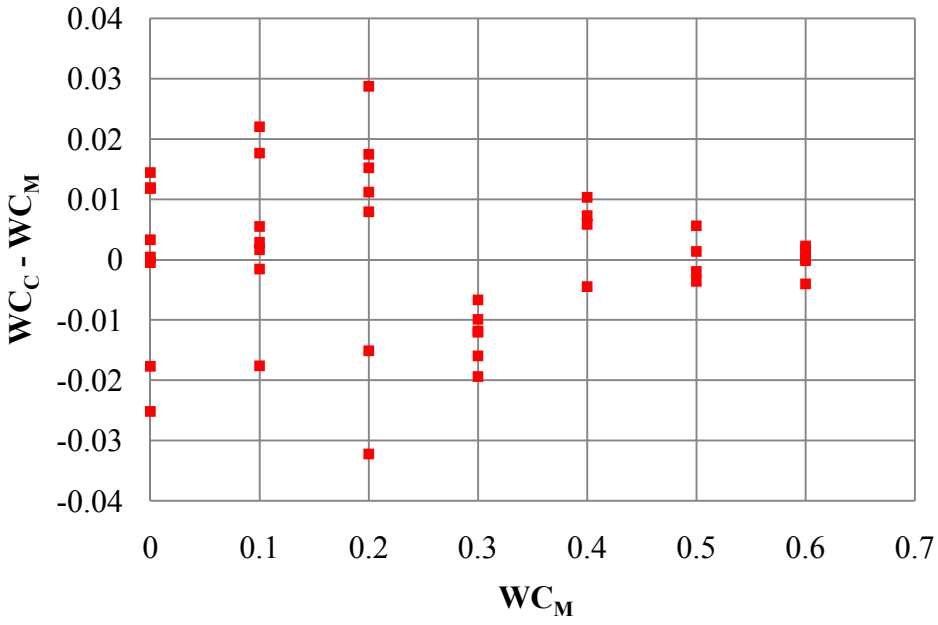


**Figure 19.** Calculated and measured watercut difference for water-in-oil

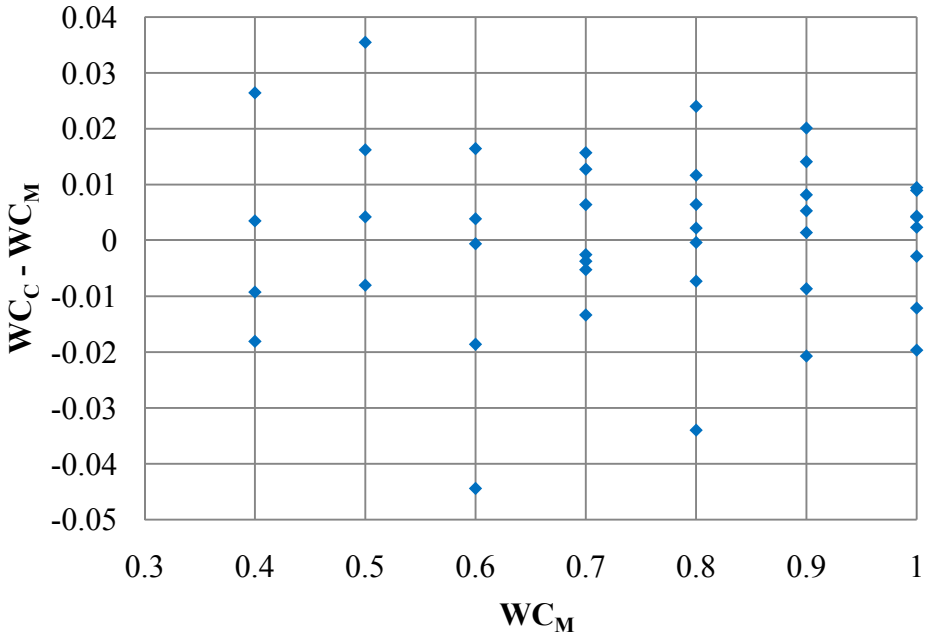


**Figure 20.** Calculated and measured watercut difference for oil-in-water

## 5.3. Mixture Resistance and Capacitance Calculation Results

The results of the resistance and capacitance calculation for the mixture at 1.28 MHz are shown in Figs. 21, 22, and 23. Fig. 22 displays the resistance for higher watercuts. The resistance is high where the continuous phase is oil and it is low where the continuous phase is water and the capacitance is high for water as the continuous phase and low for oil as the continues phase. The Figs. 21 and 22 represent that the resistance of the mixture decreases by decreasing the watercuts: however, there are significant difference between water-in-oil and oil-in-water dispersion resistance values.

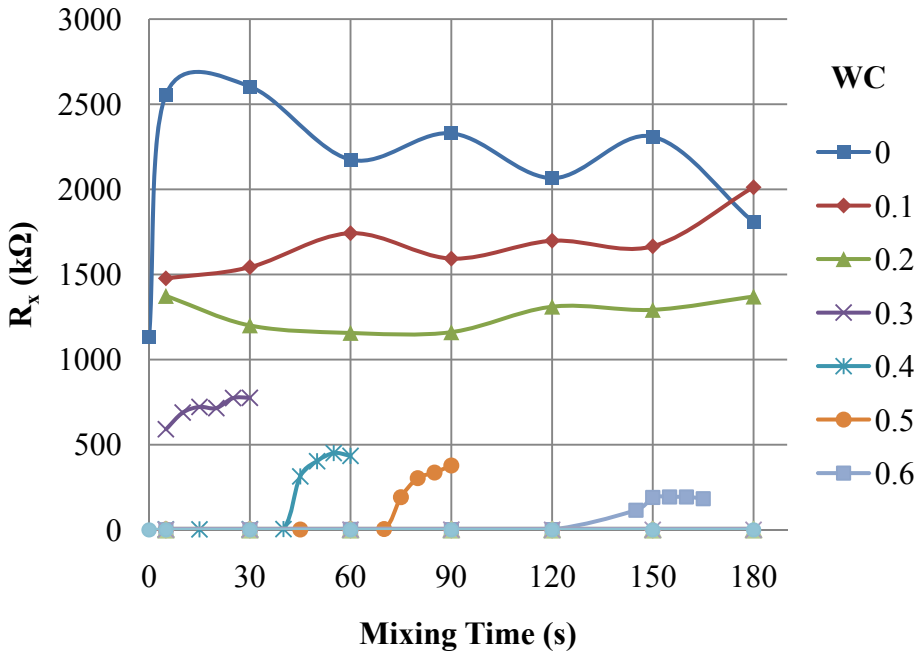


**Figure 21.** Mixture resistance for different watercuts

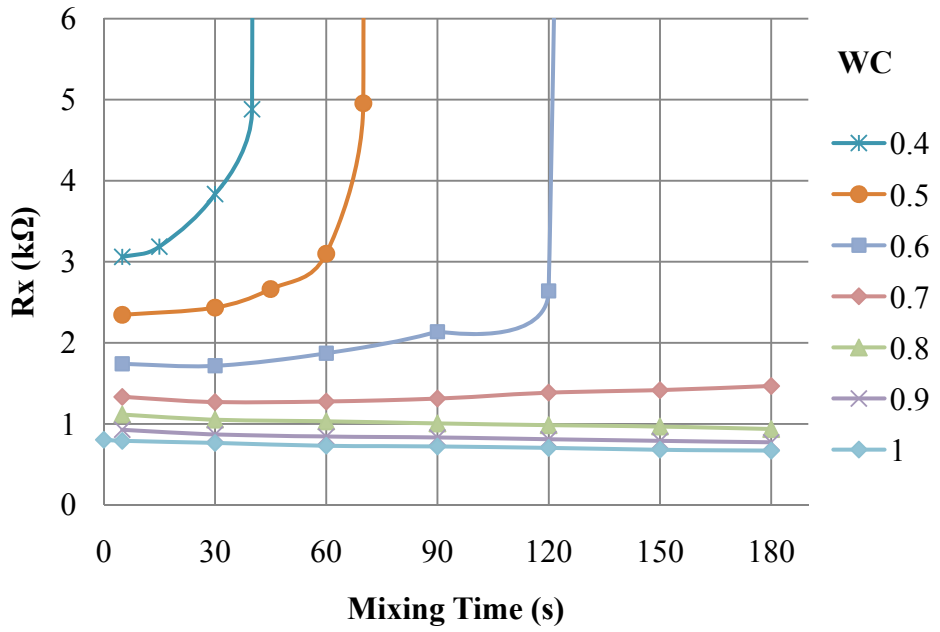


**Figure 22.** Mixture resistance detail for higher watercuts

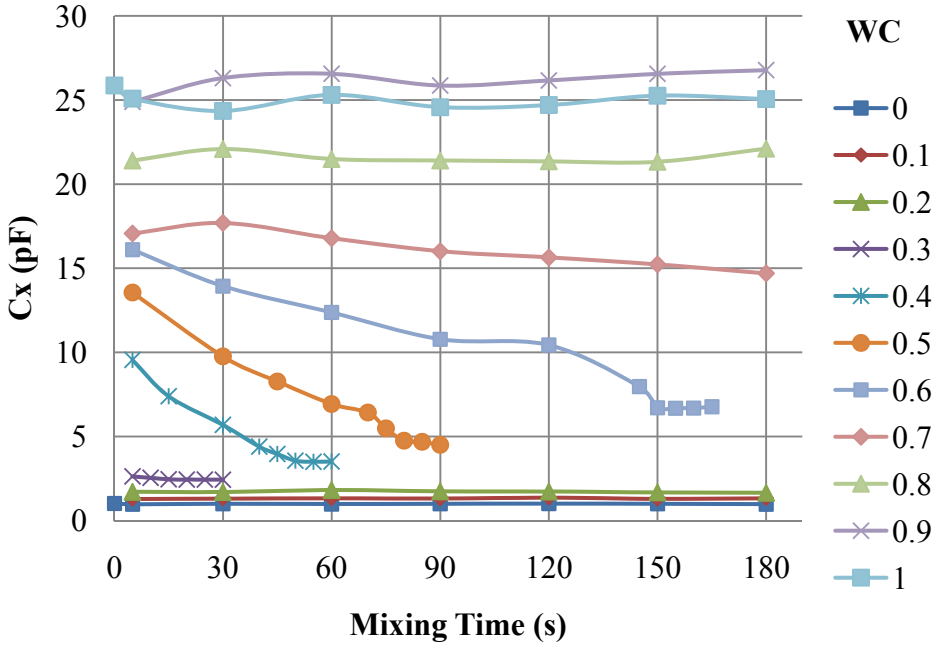


**Figure 23.** Mixture capacitance for different watercuts

The resistance and capacitance are almost constant for high and low watercuts. However, the resistance values increase and capacitance values decrease by mixing time in ambivalent range. After phase inversion, the values become constant for water-in-oil dispersion.

### 5.4. Hysteresis Effect

In this experiment, different watercut values were obtained by gradually adding water into the continuous phase of oil or oil into the continuous phase of water. Ten second mixing time and 777 rpm mixing speed were used to agitate the samples with different watercut values. The result of the hysteresis effect experiment is shown in Fig. 24. The sensor response while oil was added into water is different with respect to the case while water was added into oil due to the changes in the continuous phase. According to Fig. 24, during the process shown with the green line, the phase inversion was determined to occur.

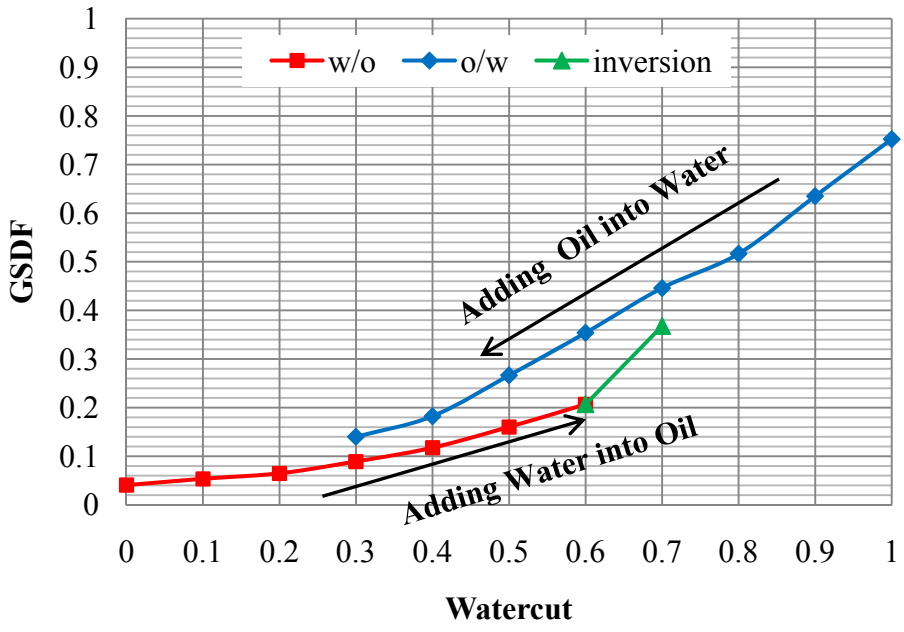


(a)

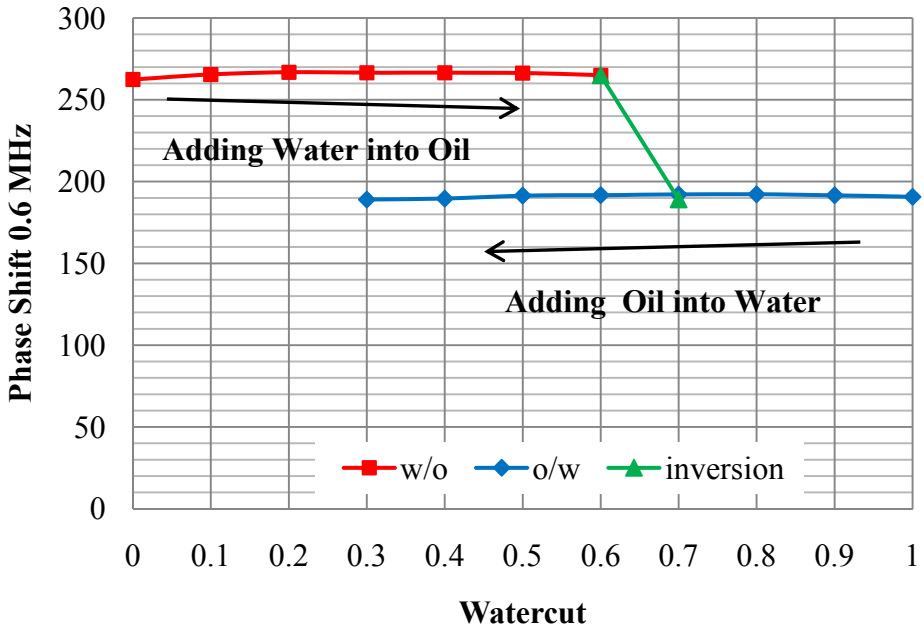


(b)

**Figure 24.** Hysteresis effect (a) GSDF and (b) 0.6 MHz phase shift results

The results from the performed study on emulsion properties and hysteresis effect are compared on Fig. 25. The W/O and O/W results are from the emulsion properties experiment and “adding water” and “adding oil” results are from hysteresis effect experiment. To provide better comparison between two experimental results, 5 s mixing time data were used as the emulsion properties result. The figure shows that the results are matched well which represents that the hysteresis does not have significant effect on the watercut measurement method.

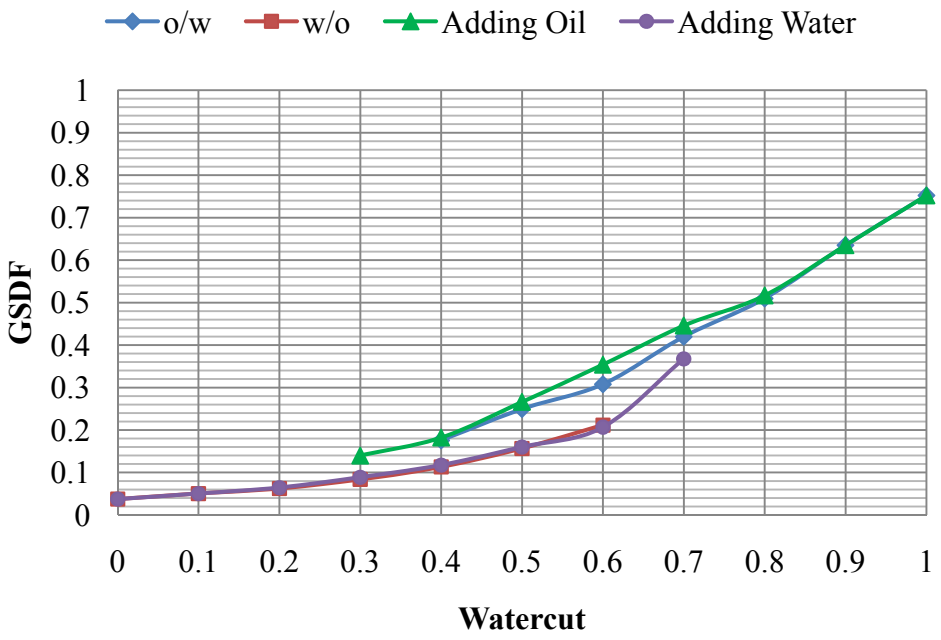


**Figure 25.** Emulsion properties and hysteresis effect comparison

## 5.5. Mixture Temperature Effect

In this study, all the experiments are started with 22.77 ºC (73 ºF) mixture temperature for emulsion properties and hysteresis effect investigation. However, the

mixture temperature increased slightly with mixing time. In this part of study, the temperature effect is investigated using water. The same amount of water (200 ml) was placed in the agitated vessel at 29.44 ºC (85 ºF). Measurements we made at different temperature till 23.88 ºC (75 ºF). The GSDF values are shown in Fig. 26 which is almost same with a watercut of 1 for 22.77 ºC in Fig. 25. This means that the GSDF values are same for different temperatures from 22.77 ºC to 29.44 ºC. This result represents that the temperature does not have significant effect on the watercut measurement method.

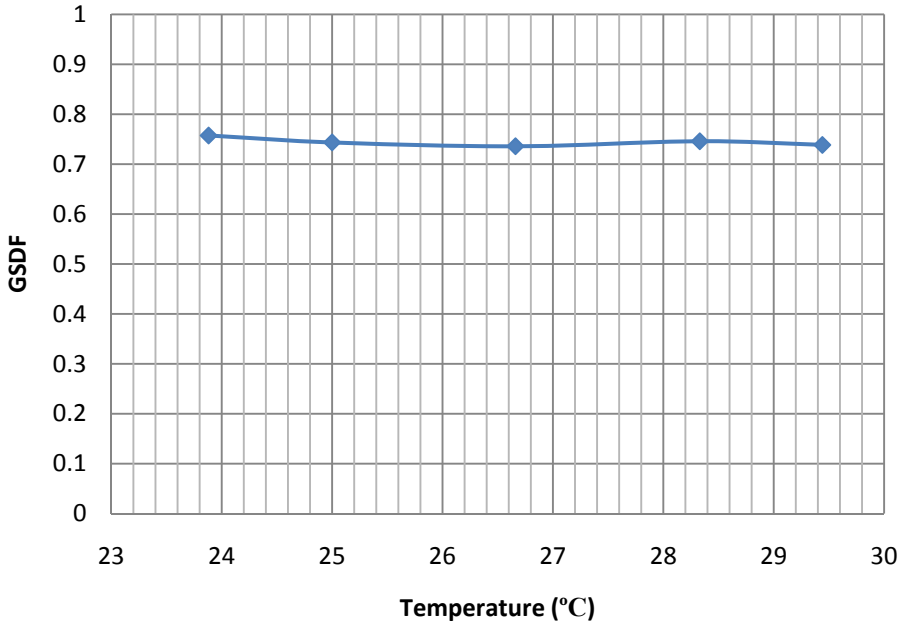


**Figure 26.** Temperature effect on watercut measurement

# 6. CONCLUSION AND RECOMMENDATIONS

## 6.1. Conclusion

In this study, the effect of shear forces on emulsion properties, hysteresis effect, and temperature effect on the response of the impedance sensor developed for watercut metering was investigated in an agitated vessel. The effect of the shear forces on emulsion properties was investigated for all watercuts separately. The sensor was found to be sensitive to shear forces effect on emulsion properties of oil-water mixture specifically in the ambivalent range. In this region, the sensor response demonstrates a noticeable variation with mixing times. Further agitation in this region leads to phase inversion in the emulsion. A new parameter was defined to reduce the dependency of the sensor response to these influencing factors. It was found that a newly developed algorithm reduces the sensitivity of the sensor response to emulsion properties specifically in this region.

The uncertainty for watercut measurement employing this method was found to be about $\pm$3% for the entire range from 0 to 1 watercut values. Resistance and capacitance of the mixture were calculated by using the gain and phase shift of the sensor. Finally, hysteresis effect was investigated by testing from 1 to 0.3 watercuts and 0 to 0.7 watercuts, and temperature effects were investigated by testing from 29.44 ºC (85 ºF) to 23.88 ºC (75 ºF) for 1 watercut. It was found that they do not have significant effect on the watercut measurement by employing the newly developed algorithm.

## 6.2. Recommendations

Recommendations for the future work are listed below:

- Ambivalent range can be investigated more especially after phase inversion
- The watercut measurement method can be tested for different oil type.
- The watercut measurement method can be tested for pipe flow.

# REFERENCES


[1] Falcone, G., Hewitt, G., & Alimonti, C. (2009). Multiphase flow metering: principles and applications (Vol. 54). (1st ed.). Oxford: UK. Elsevier.

[2] Liu, L., Matar, O. K., Susana Perez de Ortiz, E., & Hewitt, G. F. (2005). Experimental investigation of phase inversion in a stirred vessel using LIF. *Chemical Engineering Science*, 60(1), 85-94.

[3] Selker, A. H., & Sleicher, C. A. (1965). Factors affecting which phase will disperse when immiscible liquids are stirred together. *The Canadian Journal of Chemical Engineering*, 43(6), 298-301.

[4] Yeo, L. Y., Matar, O. K., de Ortiz, E. P., & Hewitt, G. F. (2000). Phase inversion and associated phenomena. *Multiphase Science and Technology*, 12(1), 51-116.

[5] Norato, M. A., Tavlarides, L. L., & Tsouris, C. (1998). Phase inversion studies in liquid-liquid dispersions. *The Canadian Journal of Chemical Engineering*, 76(3), 486-494.

[6] Arashmid, M., & Jeffreys, G. V. (1980). Analysis of the phase inversion characteristics of liquid-liquid dispersions. *AIChE Journal*, 26(1), 51-55.

[7] Yeh, G. C., Haynie, F. H., & Moses, R. A. (1964). Phase-volume relationship at the point of phase inversion in liquid dispersions. *AIChE Journal*, 10(2), 260-265.

[8] Hu, B., Angeli, P., Matar, O. K., & Hewitt, G. F. (2005). Prediction of phase inversion in agitated vessels using a two-region model. *Chemical Engineering Science*, 60(13), 3487-3495.

[9] Groeneweg, F., Agterof, W. G. M., Jaeger, P., Janssen, J. J. M., Wieringa, J. A., & Klahn, J. K. (1998). On the mechanism of the inversion of emulsions. *Chemical Engineering Research and Design*, 76(1), 55-63.

[10] Kumar, S. (1996). On phase inversion characteristics of stirred dispersions. *Chemical Engineering Science*, 51(5), 831-834.

[11] Nassereddin, T., Melo, M., Al Hagin, K., Hariz, M., Raman, B., & Helal, R. (2010, November). Infra-Red Water Cut Meter Field Trial UnderTransient Conditions. *Abu Dhabi International Petroleum Exhibition and Conference* (Vol. 3, pp. 1784-1788). Abu Dhabi: UAE. Society of Petroleum Engineers.

[12] Wu, G., Sun, J., Hanbing, Q., & Dong, L. (2010, October). Experimental Research on Water-Cut Detection of Oil-Water Mixture Based on Microwave Method. *Intelligent System Design and Engineering Application (ISDEA), 2010 International Conference* (Vol. 1, pp. 701-704). Changsha: China. IEEE.

[13] Frøystein, T., Kvandal, H., & Aakre, H. (2005). Dual energy gamma tomography system for high pressure multiphase flow. *Flow Measurement and Instrumentation*, 16(2), 99-112.

[14] Liu, X., Hu, J., Xu, W., Xu, L., Xie, Z., & Li, Y. (2009, March). A new cylindrical capacitance sensor for measurement of water cut in a low-production horizontal well. *Journal of Physics: Conference Series* (Vol. 147, pp. 012002). Okinawa: Japan. IOP Publishing.

[15] Chun, M. H., & Sung, C. K. (1986). Parametric effects on the void fraction measurement by capacitance transducers. *International Journal of Multiphase Flow*, 12(4), 627-640.

[16] Merilo, M., Dechene, R. L., & Cichowlas, W. M. (1977). Void fraction measurement with a rotating electric field conductance gauge. *Journal of Heat Transfer*, 99(2), 330-332.

[17]Morrison, G., Pirouzpanah, S., Cevik, M., & Patil, A. (2013, July). Evaluation of a Close Coupled Slotted Orifice, Electric Impedance, and Swirl Flow Meters for Multiphase Flow. *ASME 2013 Fluids Engineering Division Summer Meeting* (Vol.2, pp. V002T11A002). Navada: USA. American Society of Mechanical Engineers.

[18] Gamio, J. C., Yang, W. Q., & Stott, A. L. (2001). Analysis of non-ideal characteristics of an ac-based capacitance transducer for tomography. *Measurement Science and Technology*, 12(8), 1076.

[19] Clayton, G. B., & Winder, S. (2003). Operational amplifiers. (5th ed.). London: UK. Newnes.

APPENDIX A

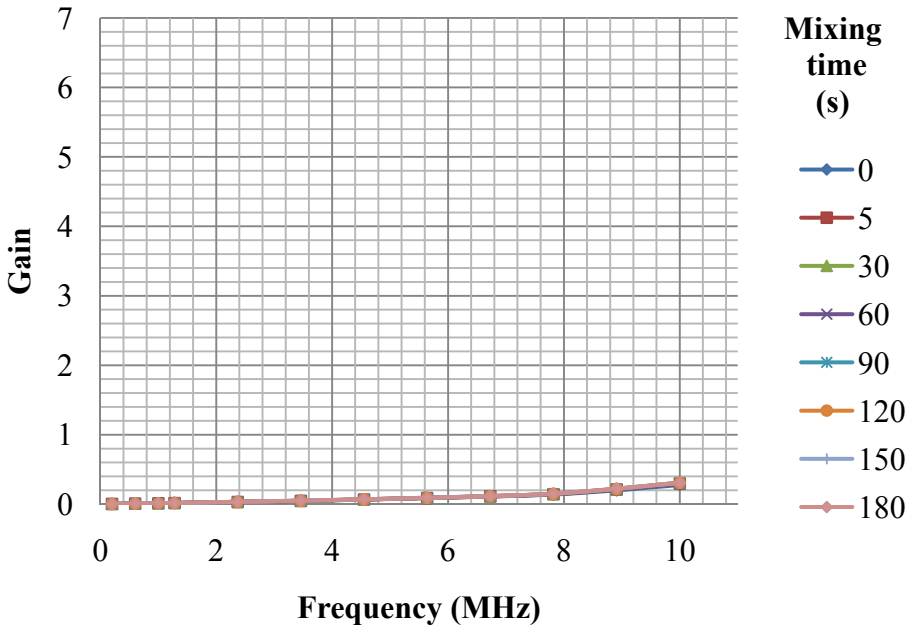


**Figure 27.** Gain variation with frequency for different mixing times at 0 watercut

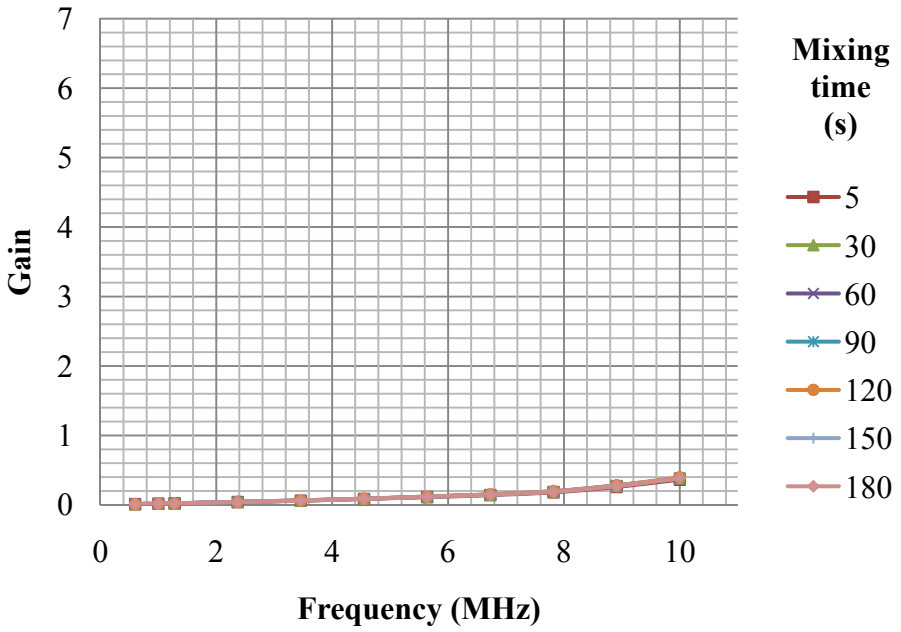


**Figure 28.** Gain variation with frequency for different mixing times at 0.1 watercut

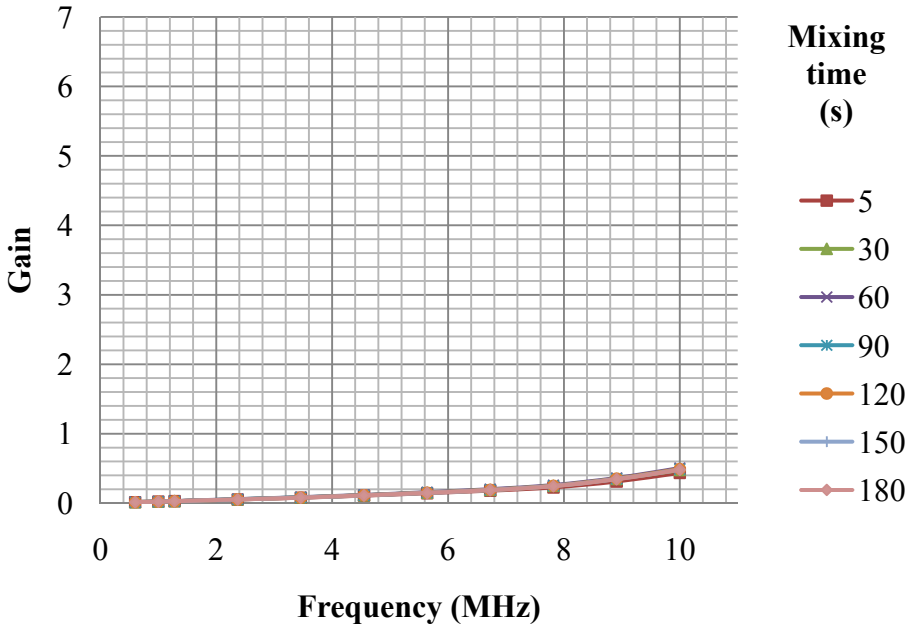


**Figure 29.** Gain variation with frequency for different mixing times at 0.2 watercut

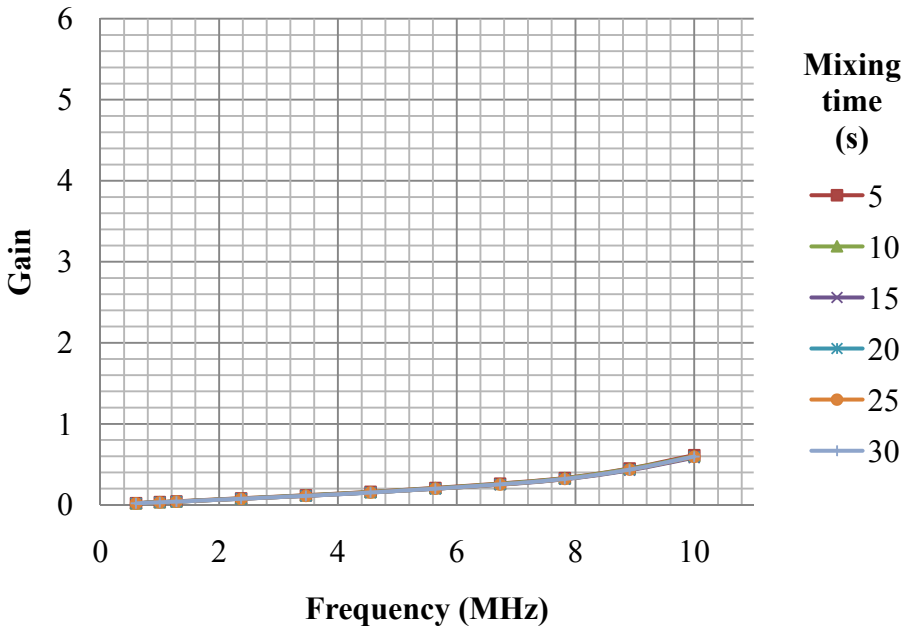


**Figure 30.** Gain variation with frequency for different mixing times at 0.3 watercut

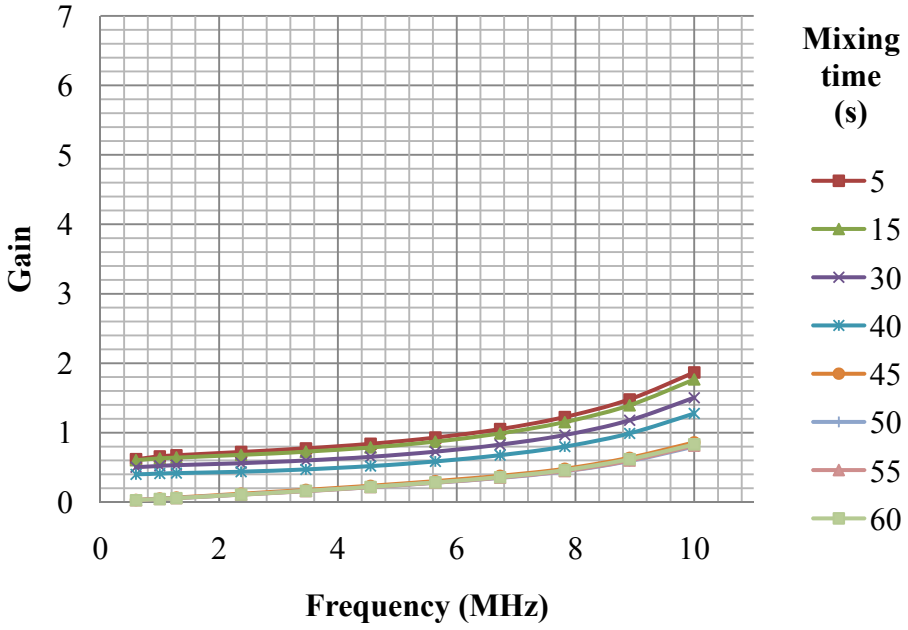


**Figure 31.** Gain variation with frequency for different mixing times at 0.4 watercut

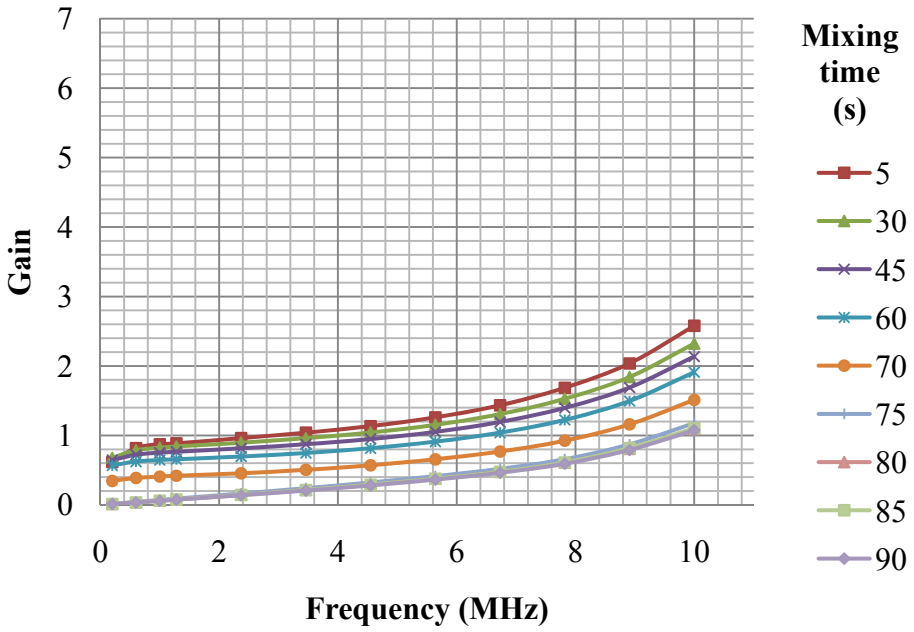


**Figure 32.** Gain variation with frequency for different mixing times at 0.5 watercut

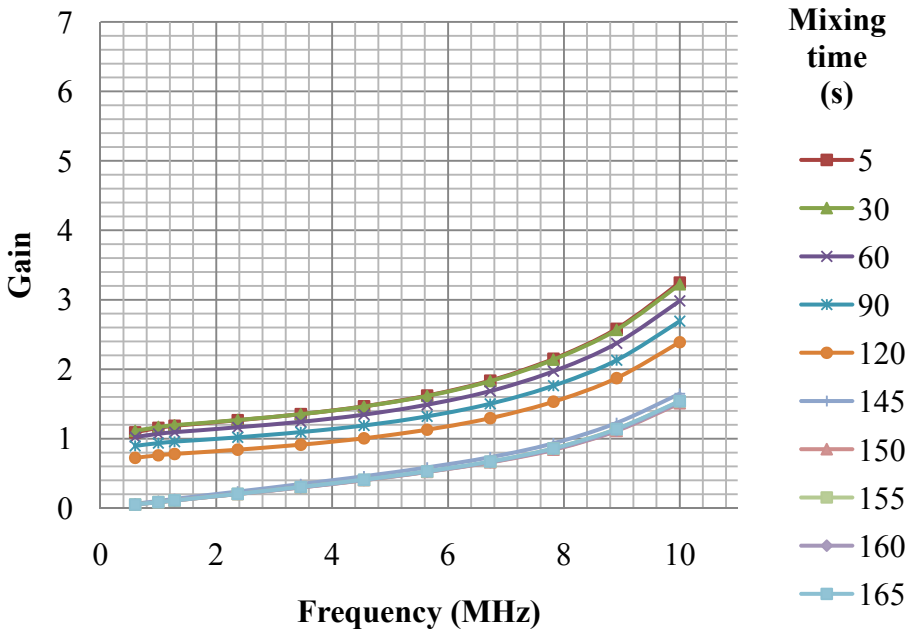


**Figure 33.** Gain variation with frequency for different mixing times at 0.6 watercut

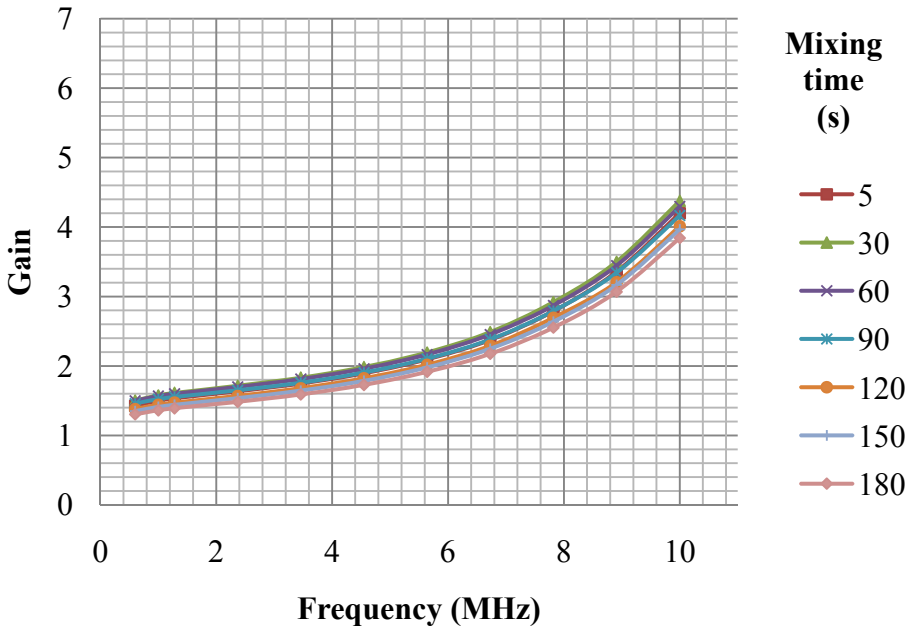


**Figure 34.** Gain variation with frequency for different mixing times at 0.7 watercut

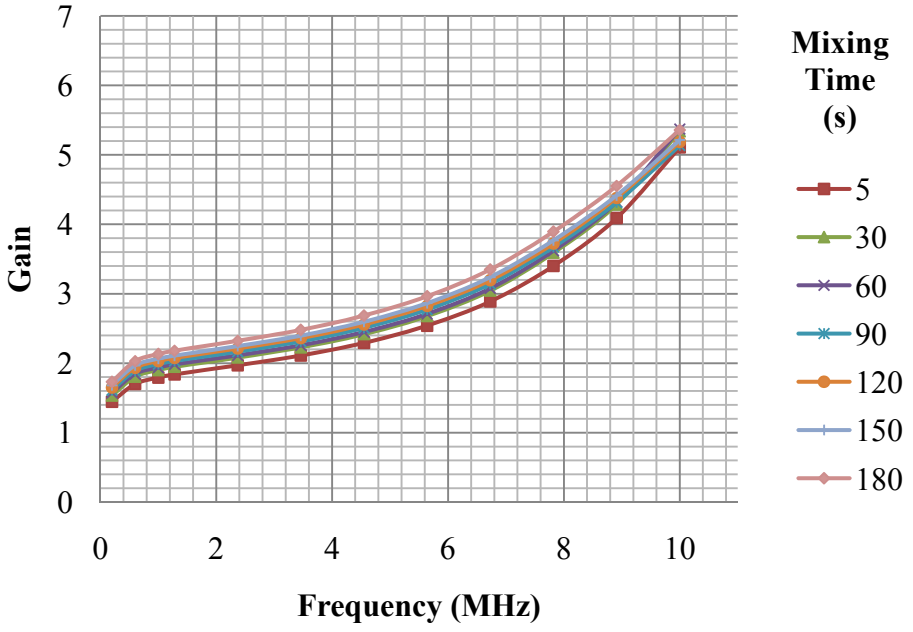


**Figure 35.** Gain variation with frequency for different mixing times at 0.8 watercut

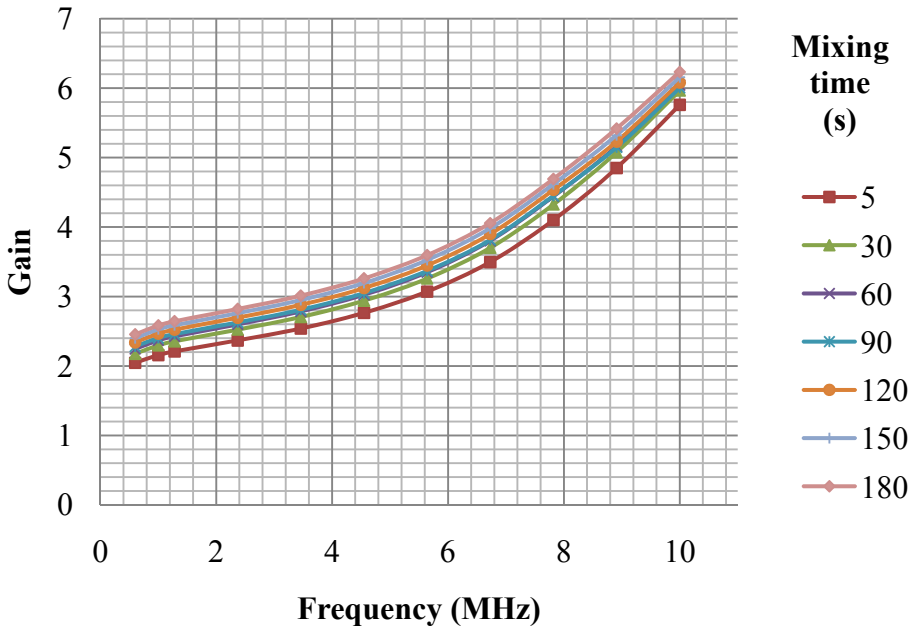


**Figure 36.** Gain variation with frequency for different mixing times at 0.9 watercut

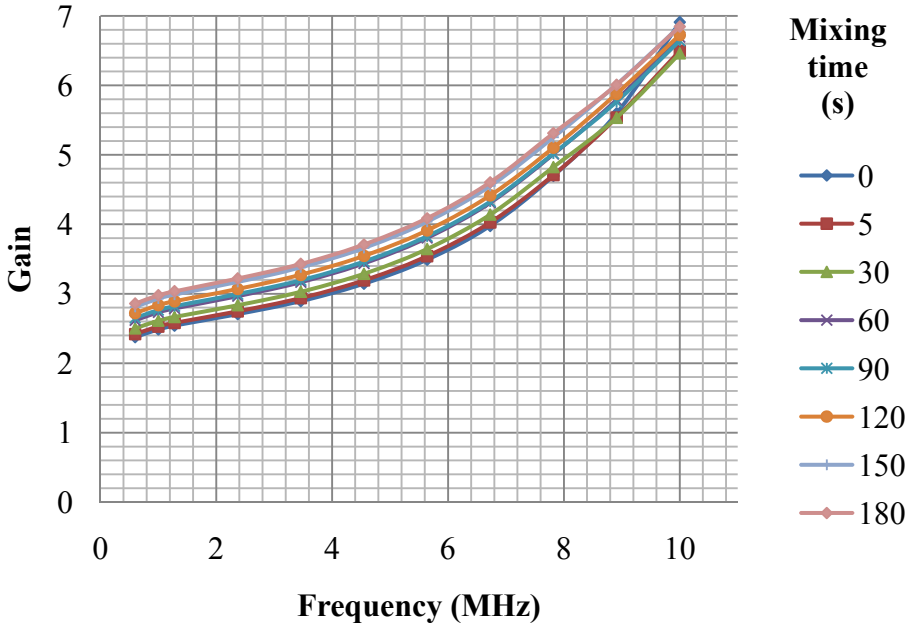


**Figure 37.** Gain variation with frequency for different mixing times at 1 watercut

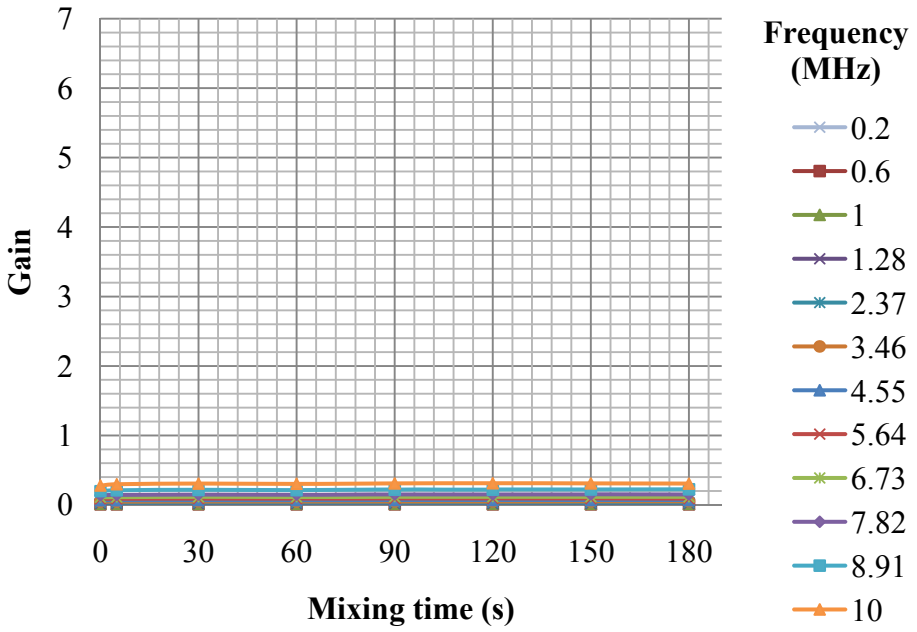


**Figure 38.** Gain variation by mixing time for different frequencies at 0 watercut

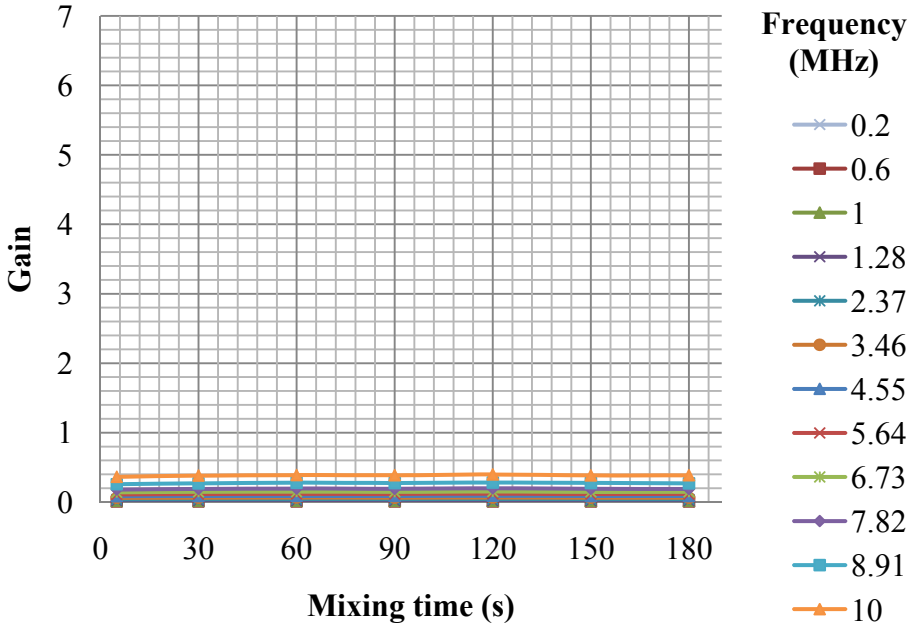


**Figure 39.** Gain variation by mixing time for different frequencies at 0.1 watercut

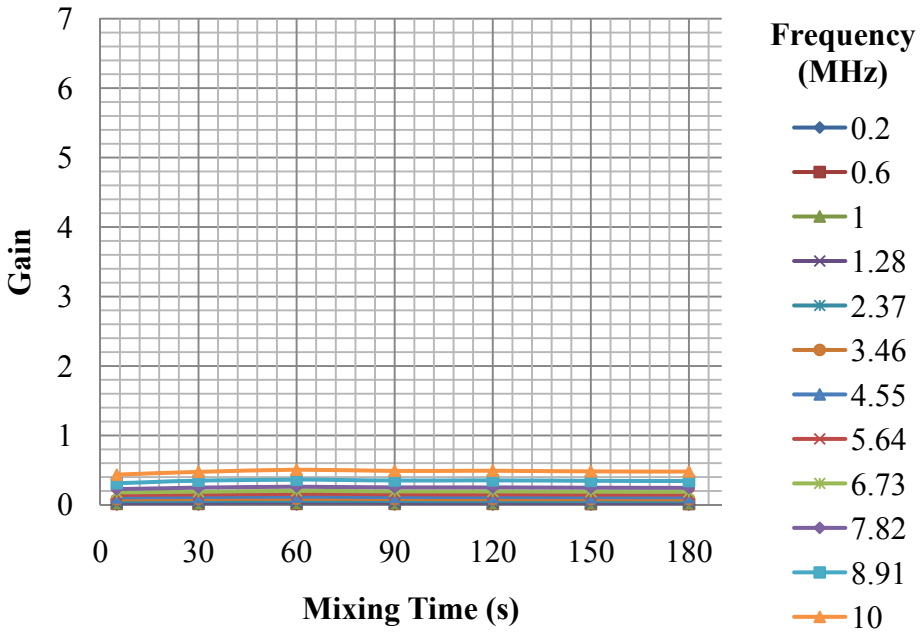


**Figure 40.** Gain variation by mixing time for different frequencies at 0.2 watercut

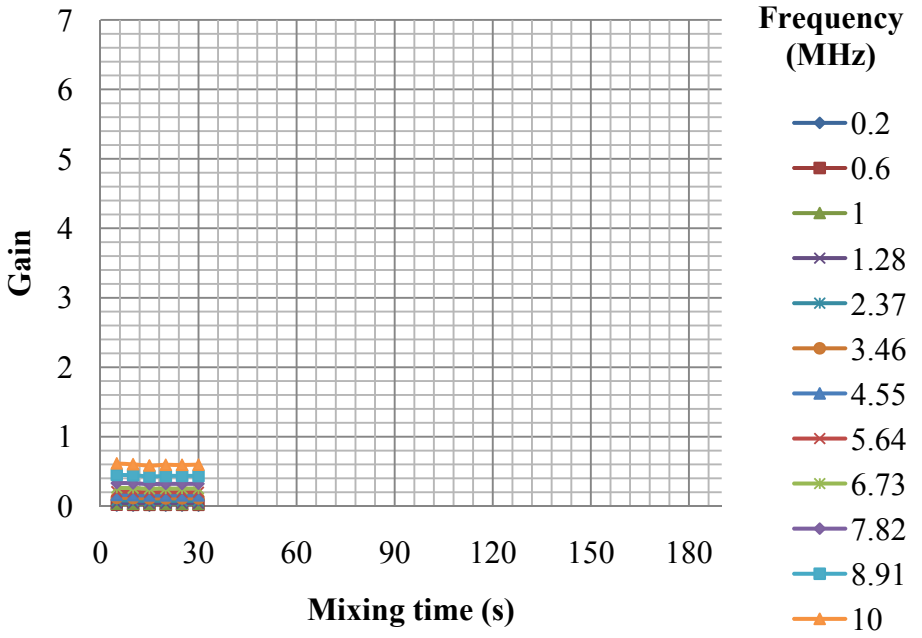


**Figure 41.** Gain variation by mixing time for different frequencies at 0.3 watercut

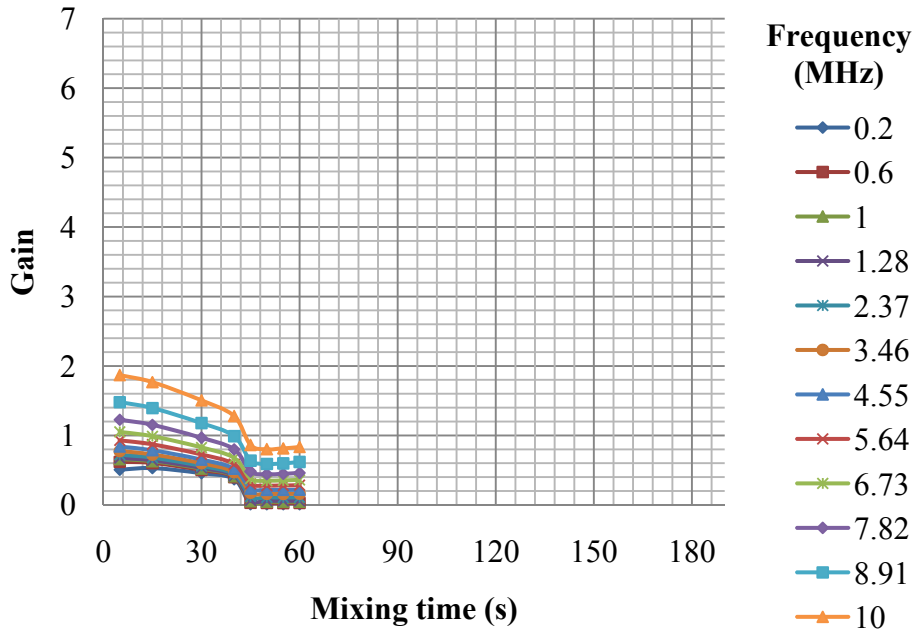


**Figure 42.** Gain variation by mixing time for different frequencies at 0.4 watercut

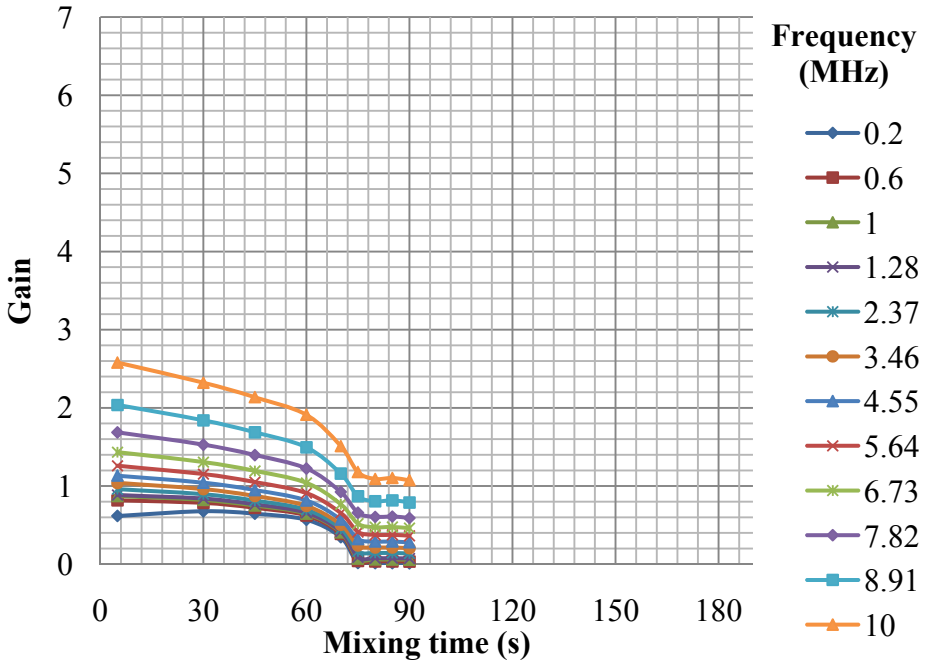


**Figure 43.** Gain variation by mixing time for different frequencies at 0.5 watercut

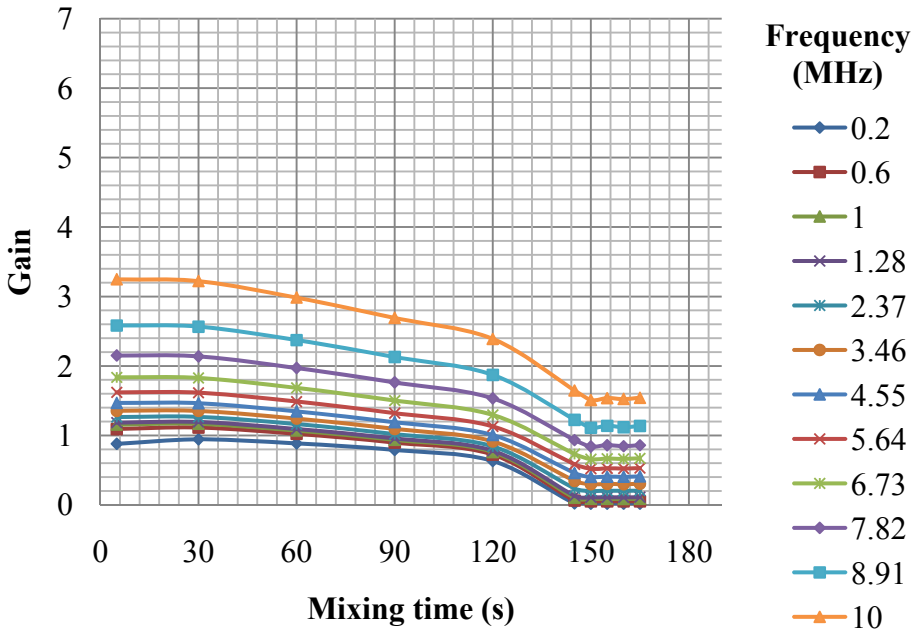


**Figure 44.** Gain variation by mixing time for different frequencies at 0.6 watercut

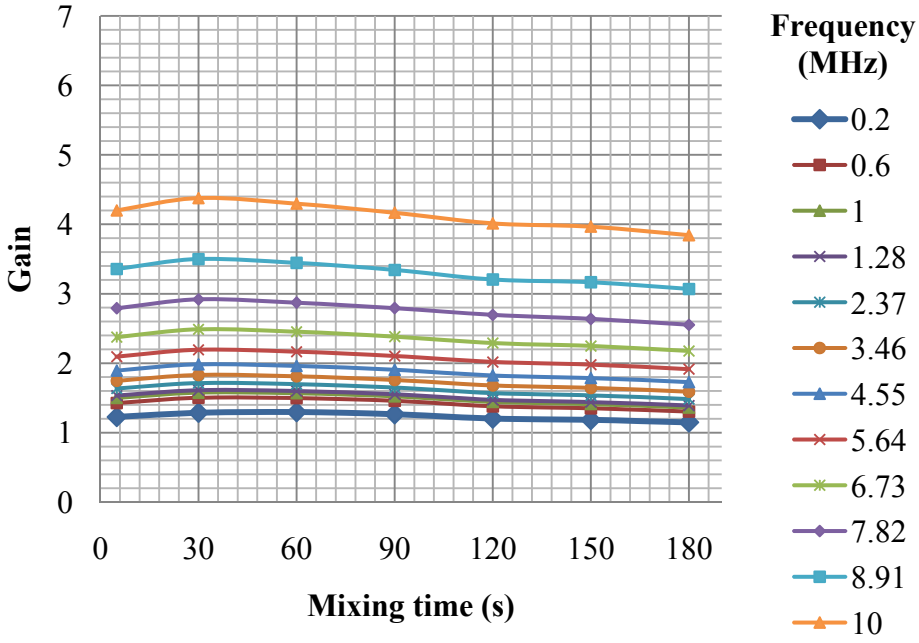


**Figure 45.** Gain variation by mixing time for different frequencies at 0.7 watercut

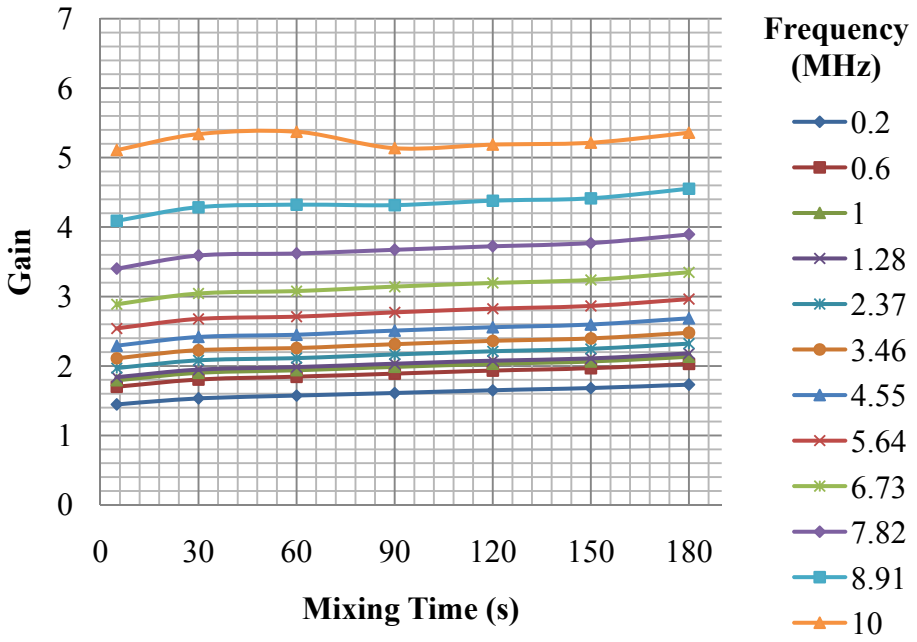


**Figure 46.** Gain variation by mixing time for different frequencies at 0.8 watercut

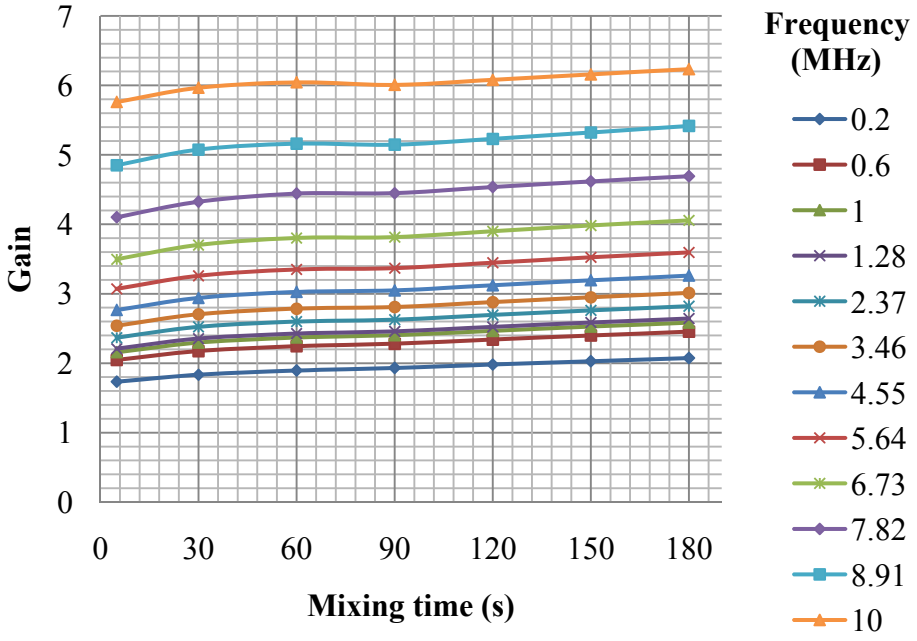


**Figure 47.** Gain variation by mixing time for different frequencies at 0.9 watercut

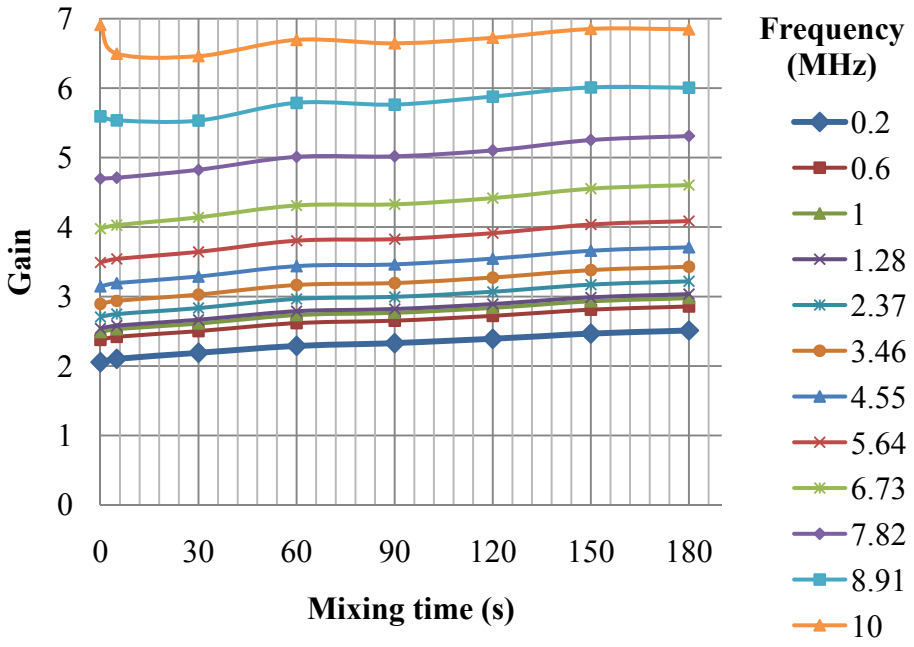


**Figure 48.** Gain variation by mixing time for different frequencies at 1 watercut

APPENDIX B

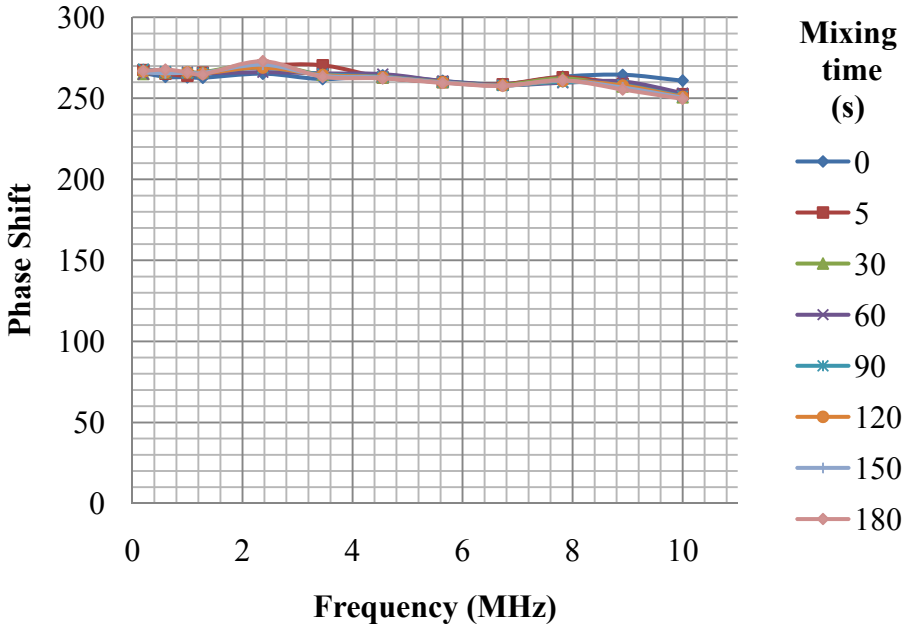


**Figure 49.** Phase shift with frequency for different mixing times at 0 watercut

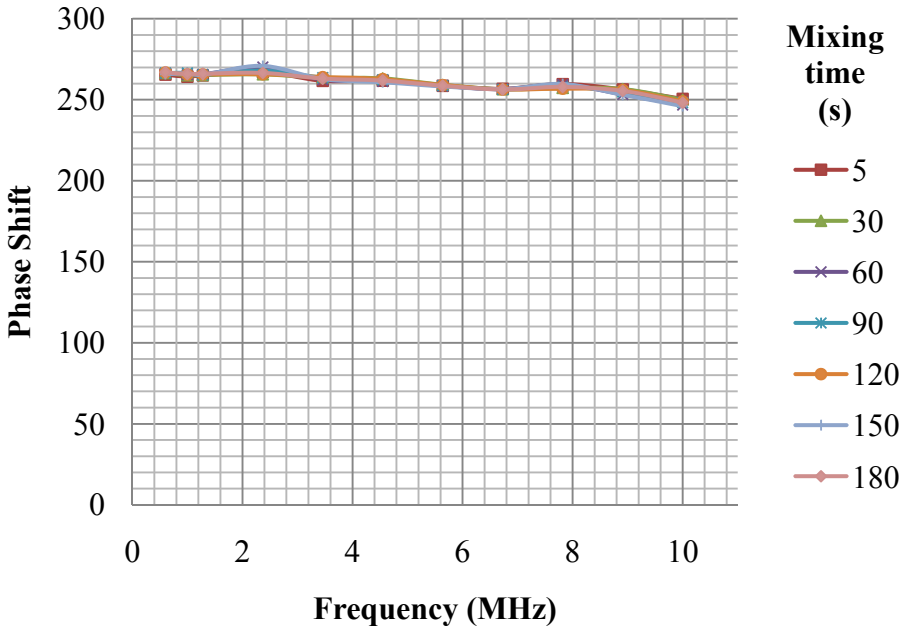


**Figure 50.** Phase shift with frequency for different mixing times at 0.1 watercut

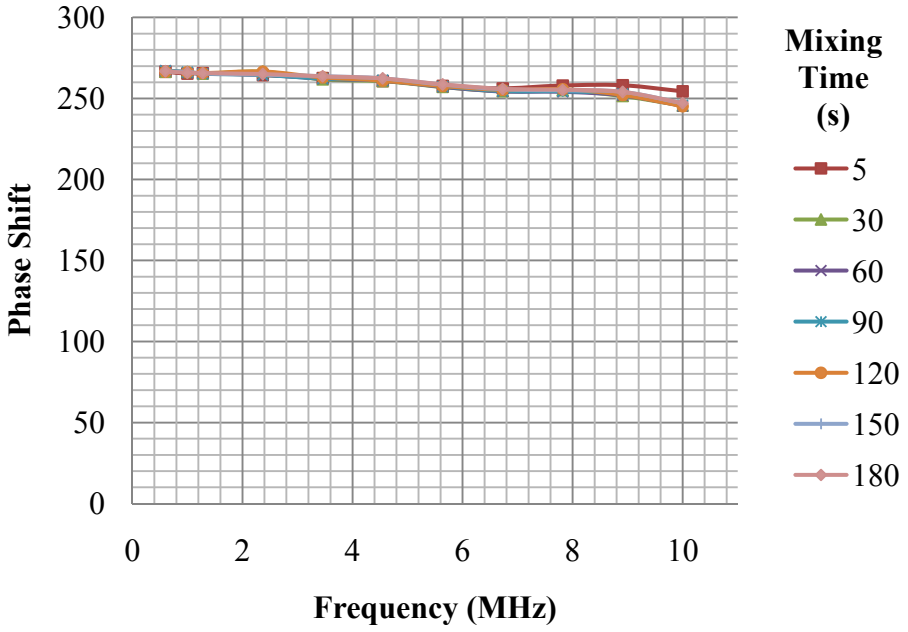


**Figure 51.** Phase shift with frequency for different mixing times at 0.2 watercut

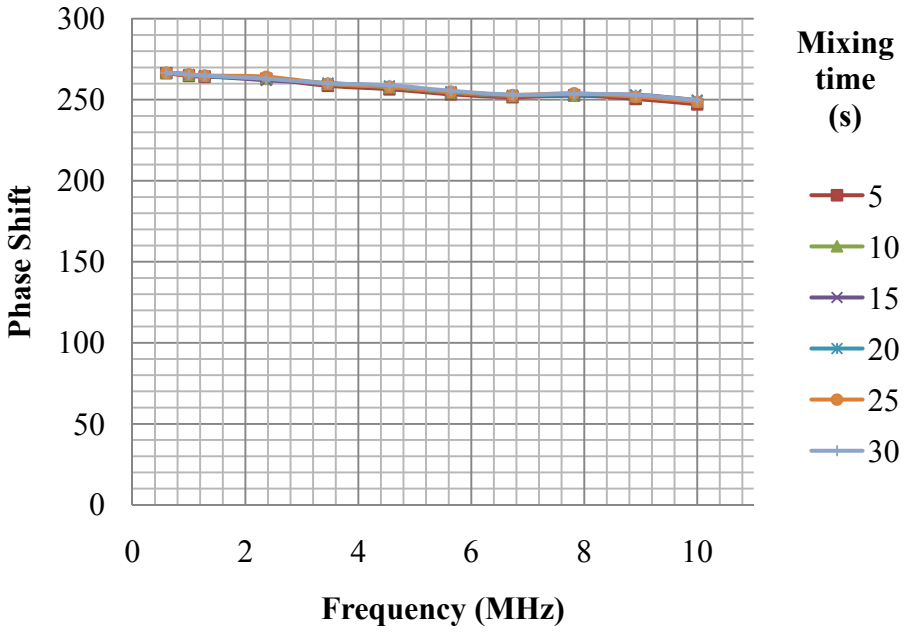


**Figure 52.** Phase shift with frequency for different mixing times at 0.3 watercut

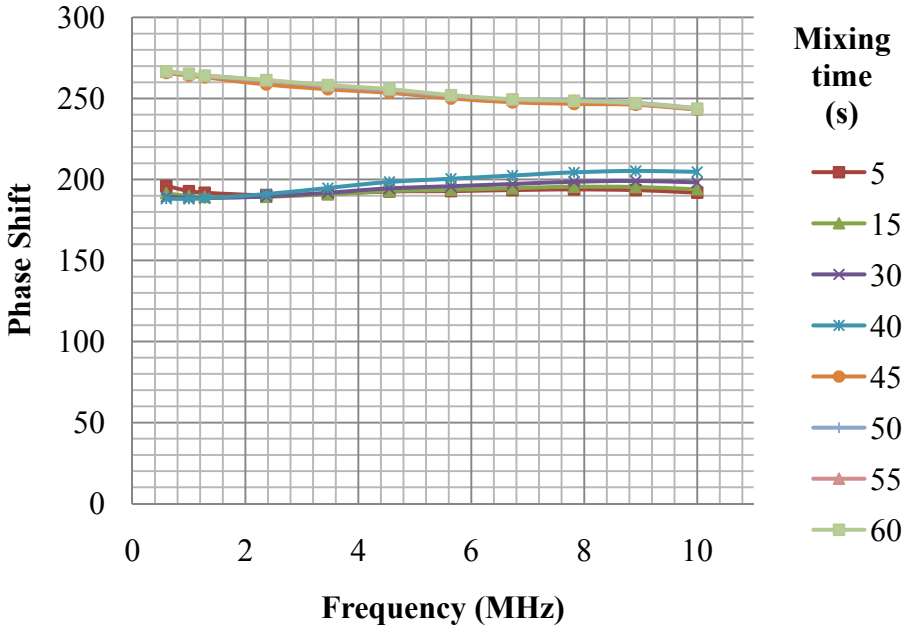


**Figure 53.** Phase shift with frequency for different mixing times at 0.4 watercut

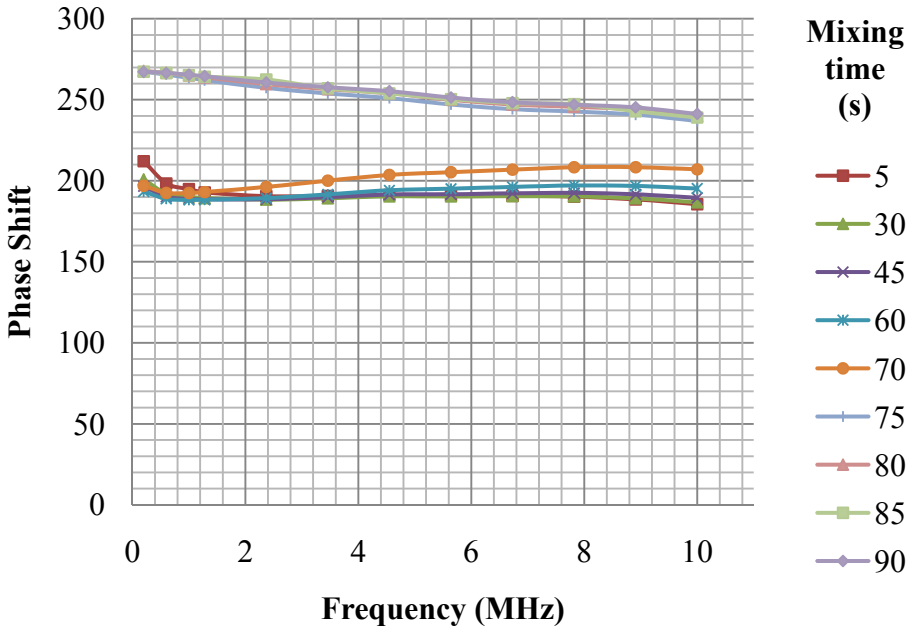


**Figure 54.** Phase shift with frequency for different mixing times at 0.5 watercut

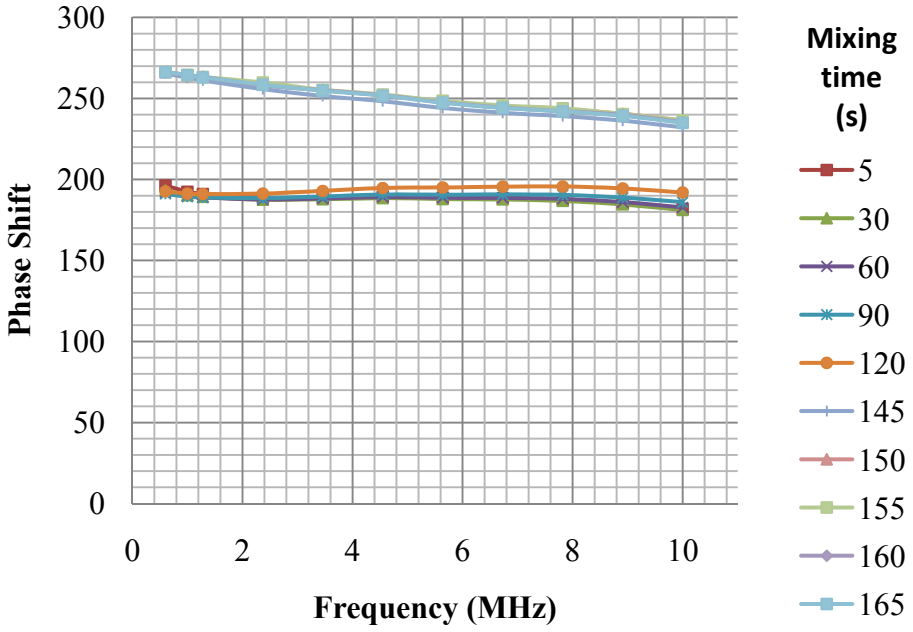


**Figure 55.** Phase shift with frequency for different mixing times at 0.6 watercut

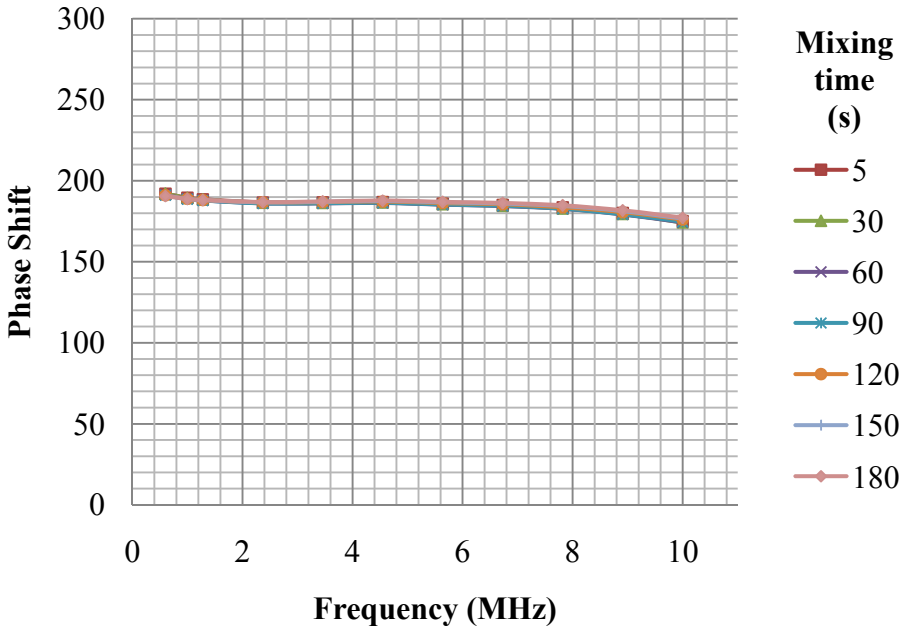


**Figure 56.** Phase shift with frequency for different mixing times at 0.7 watercut

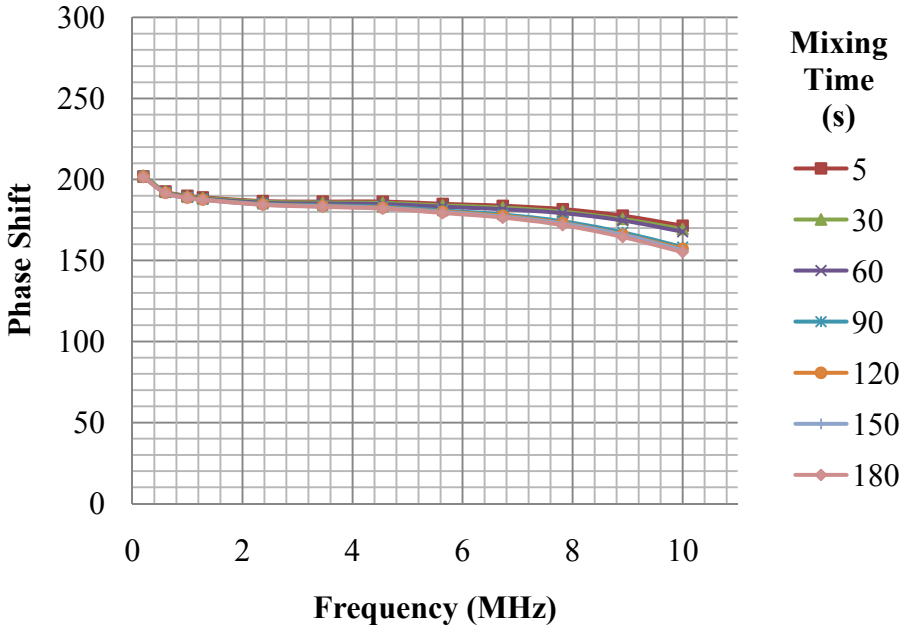


**Figure 57.** Phase shift with frequency for different mixing times at 0.8 watercut

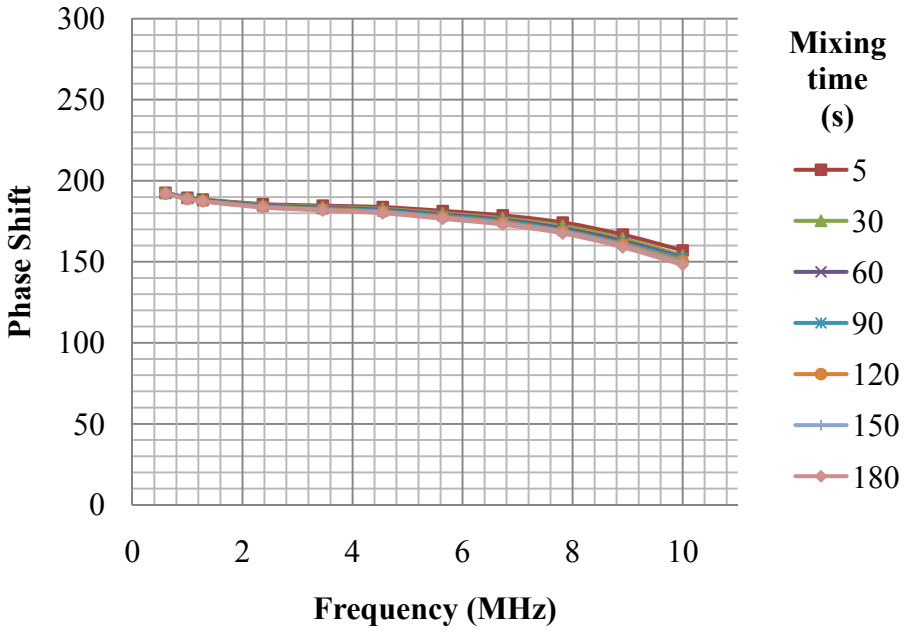


**Figure 58.** Phase shift with frequency for different mixing times at 0.9 watercut

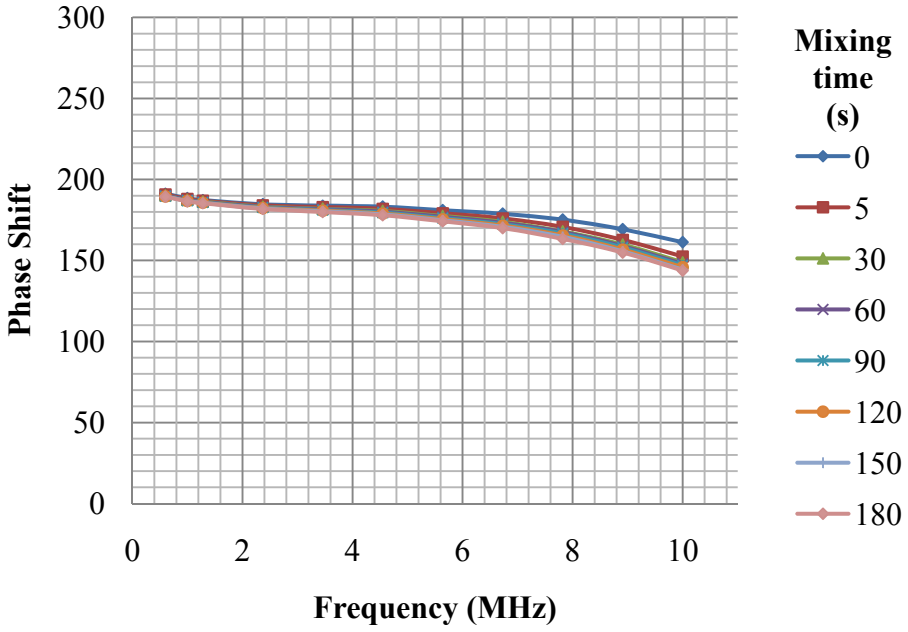


**Figure 59.** Phase shift with frequency for different mixing times at 1 watercut

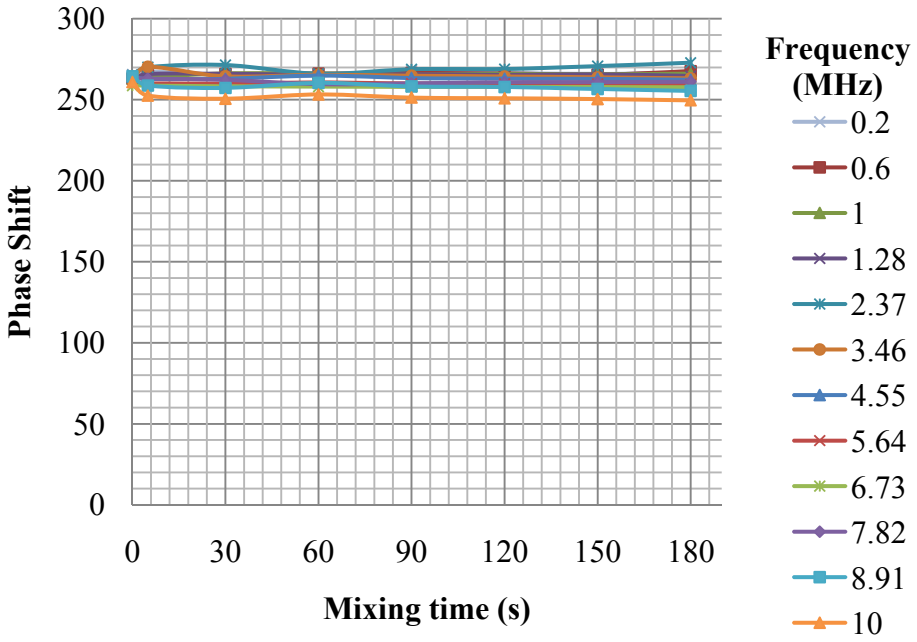


**Figure 60.** Phase shift by mixing time for different frequencies at 0 watercut

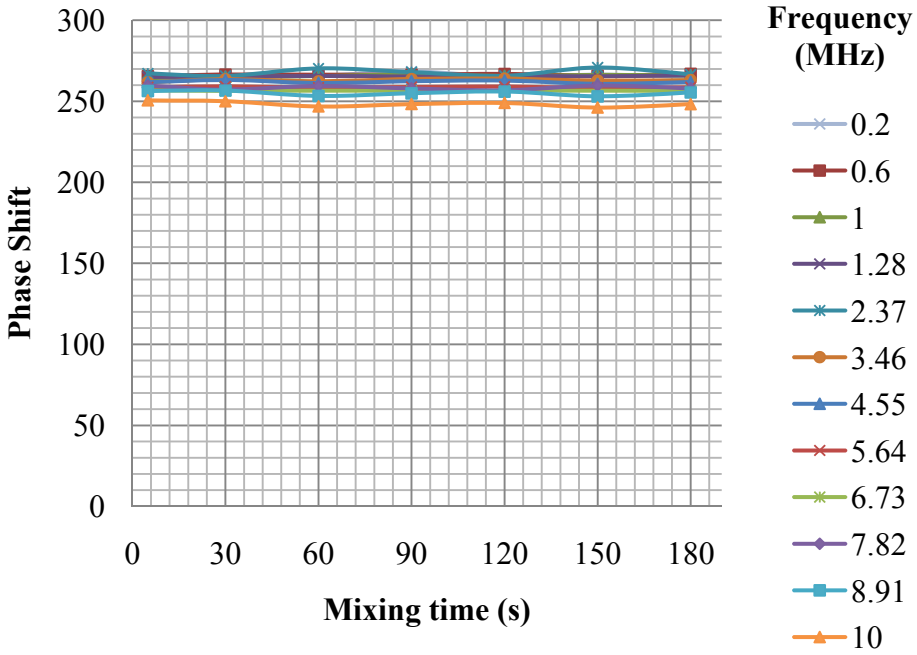


**Figure 61.** Phase shift by mixing time for different frequencies at 0.1 watercut

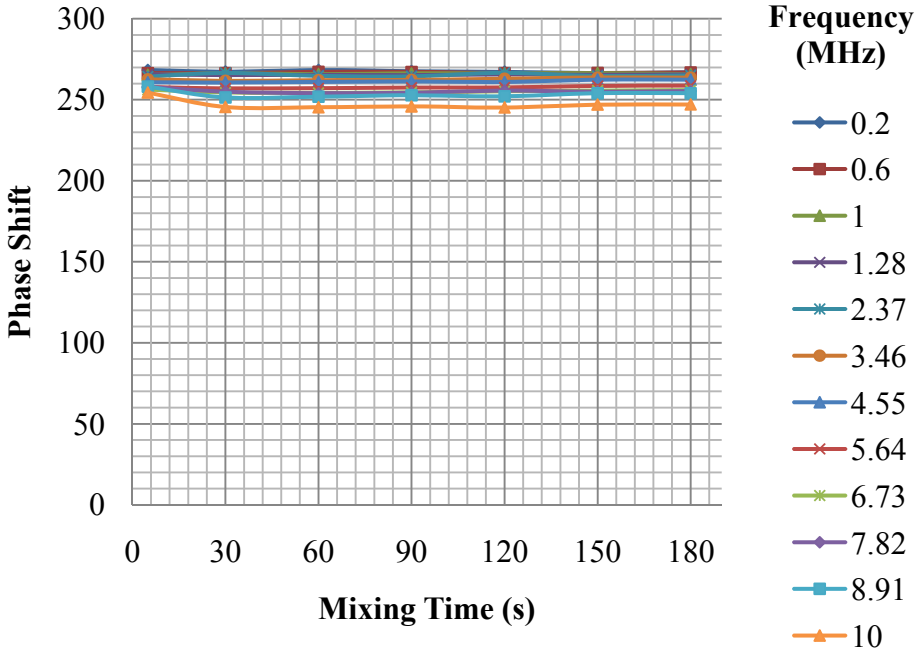


**Figure 62.** Phase shift by mixing time for different frequencies at 0.2 watercut

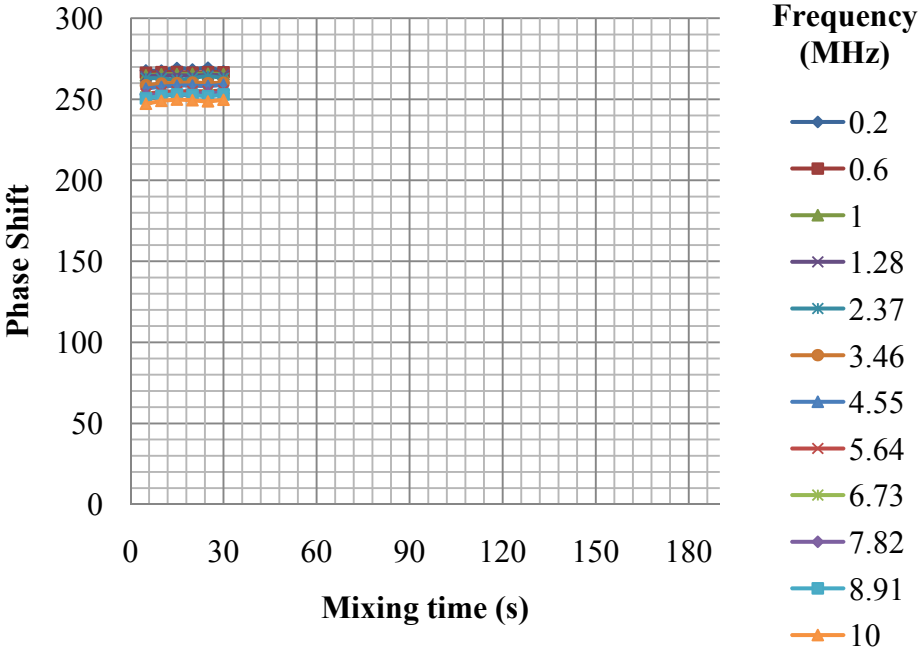


**Figure 63.** Phase shift by mixing time for different frequencies at 0.3 watercut

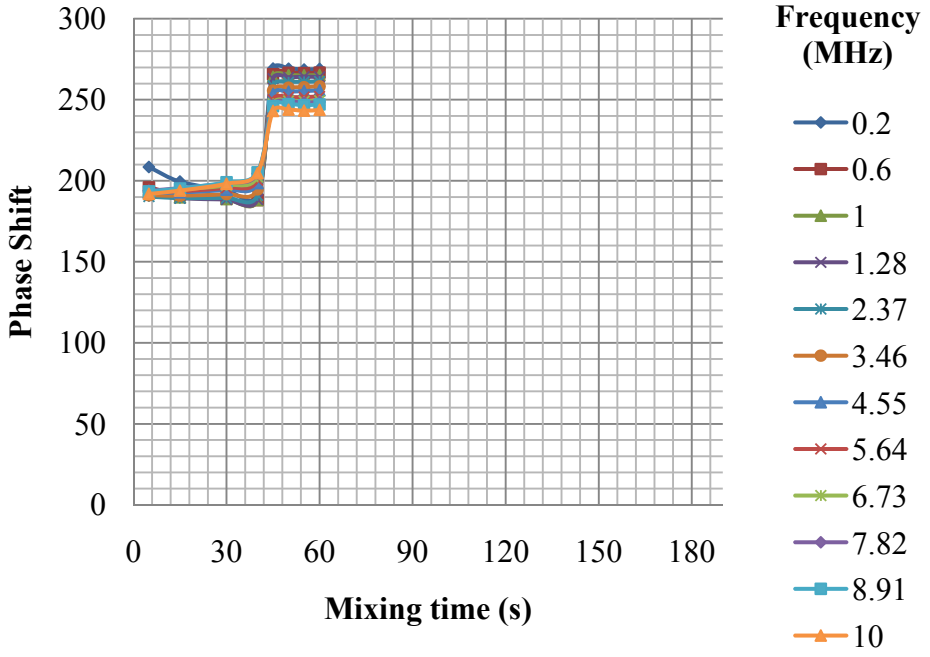


**Figure 64.** Phase shift by mixing time for different frequencies at 0.4 watercut

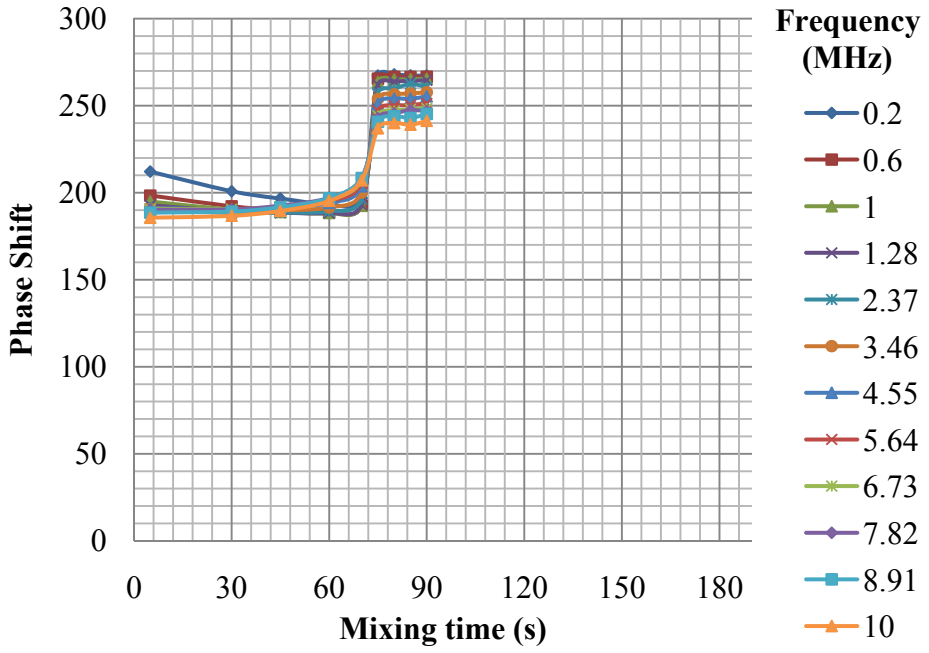


**Figure 65.** Phase shift by mixing time for different frequencies at 0.5 watercut

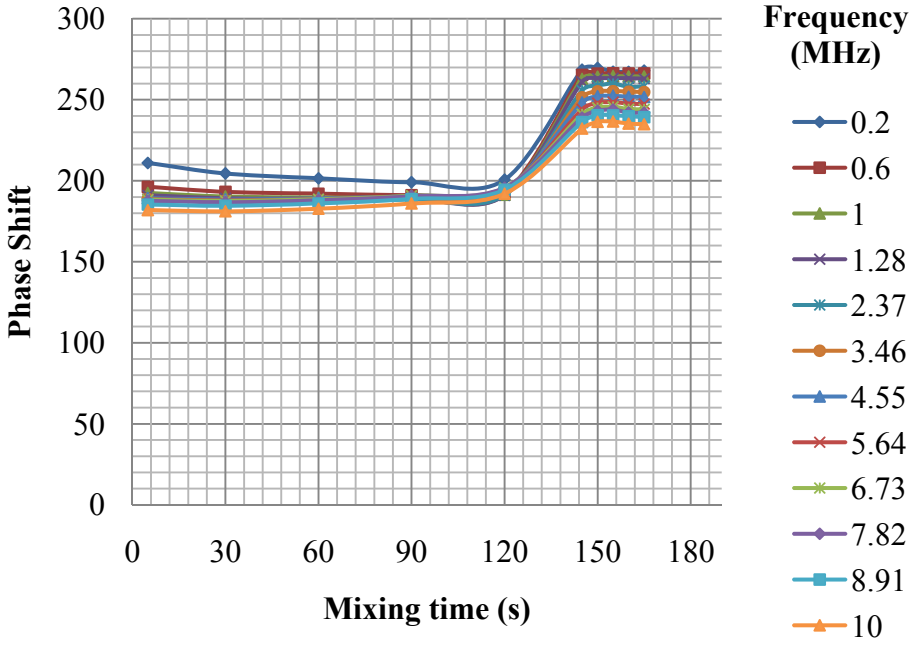


**Figure 66.** Phase shift by mixing time for different frequencies at 0.6 watercut

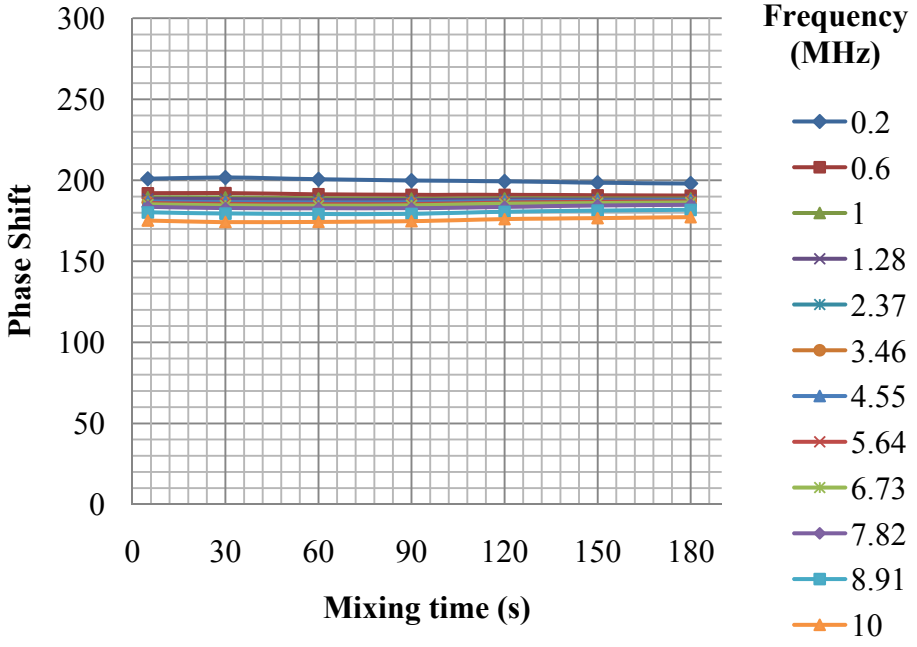


**Figure 67.** Phase shift by mixing time for different frequencies at 0.7 watercut

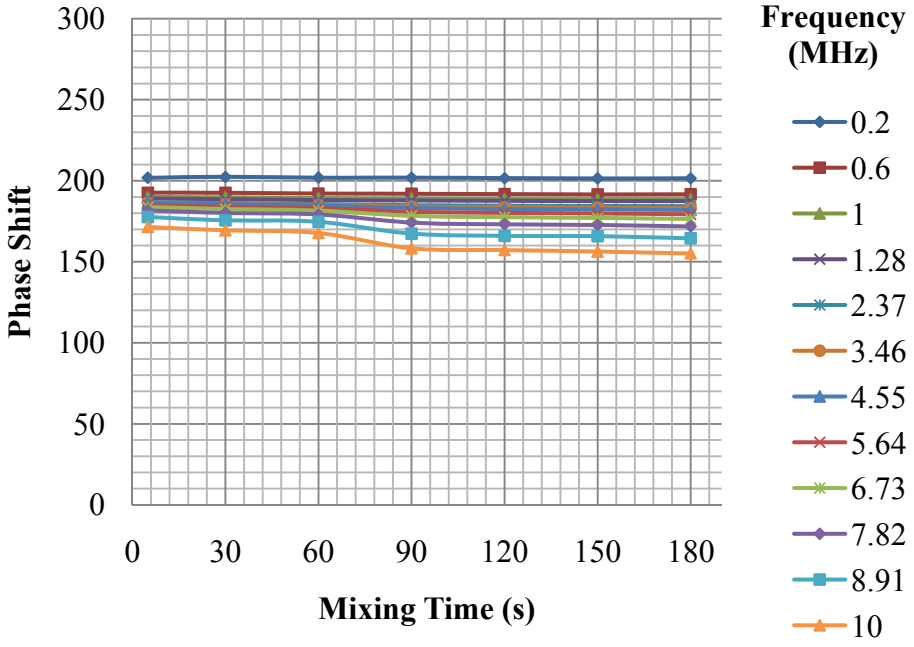


**Figure 68.** Phase shift by mixing time for different frequencies at 0.8 watercut

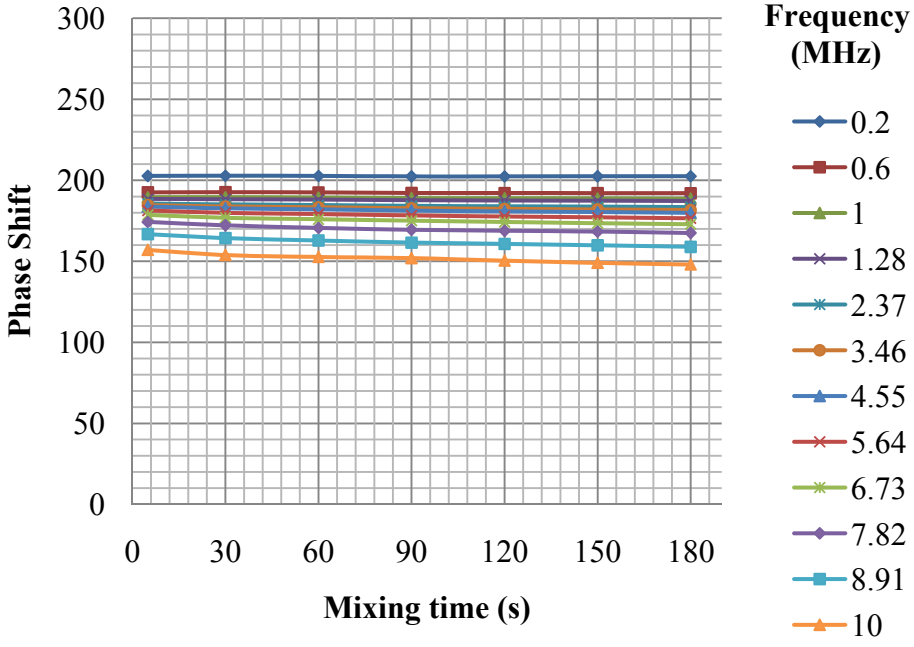


**Figure 69.** Phase shift by mixing time for different frequencies at 0.9 watercut

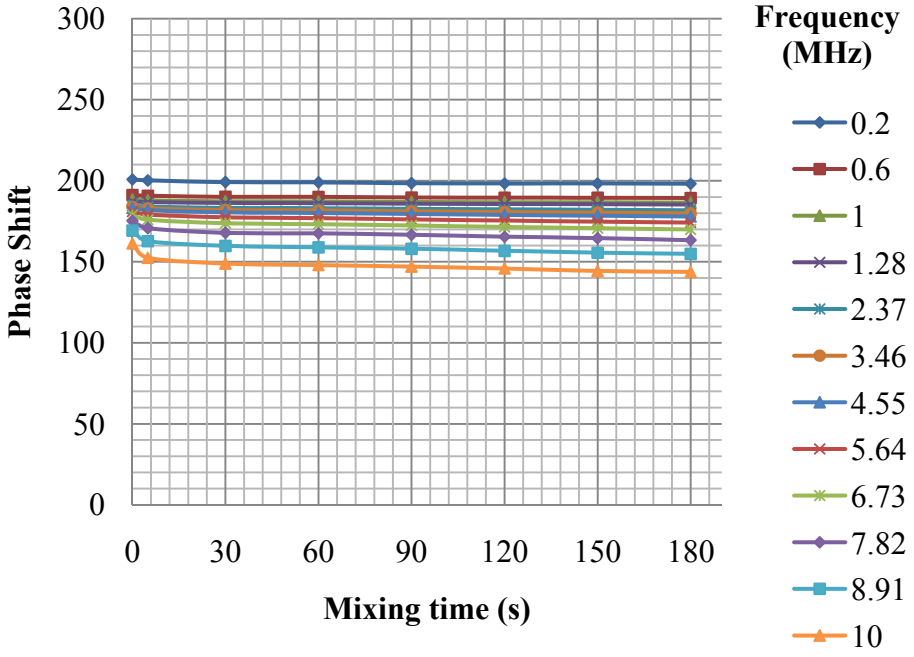


**Figure 70.** Phase shift by mixing time for different frequencies at 1 watercut

APPENDIX C

**Table 3.** Test Matrix

| **Process** | **Status** |
|---|---|
| Be sure about the vessel cleaning | |
| Measure the water amount for appropriate watercut and add into vessel | |
| Measure the oil amount for appropriate watercut and add into vessel | |
| Be sure about the sensors are connected to the circuit | |
| Turn on the power | |
| Run the Labview software | |
| Run the agitator for 5 seconds and stop it | |
| Save the data for 5 seconds | |
| Run the agitator for 25 seconds more and stop it | |
| Save the data for 30 seconds | |
| Run the agitator for 30 seconds more and stop it. | |
| Save the data for 60, 90, 120, 150, and 180 seconds | |
| In the ambivalent range, arrange the time depends on the mixture behavior | |
| Stop the Labview software | |
| Turn off the power | |
| Disconnect the sensors from the circuit | |
| Clean the vessel | |
| Run the Matlab code for the data | |
| Draw the figures | |